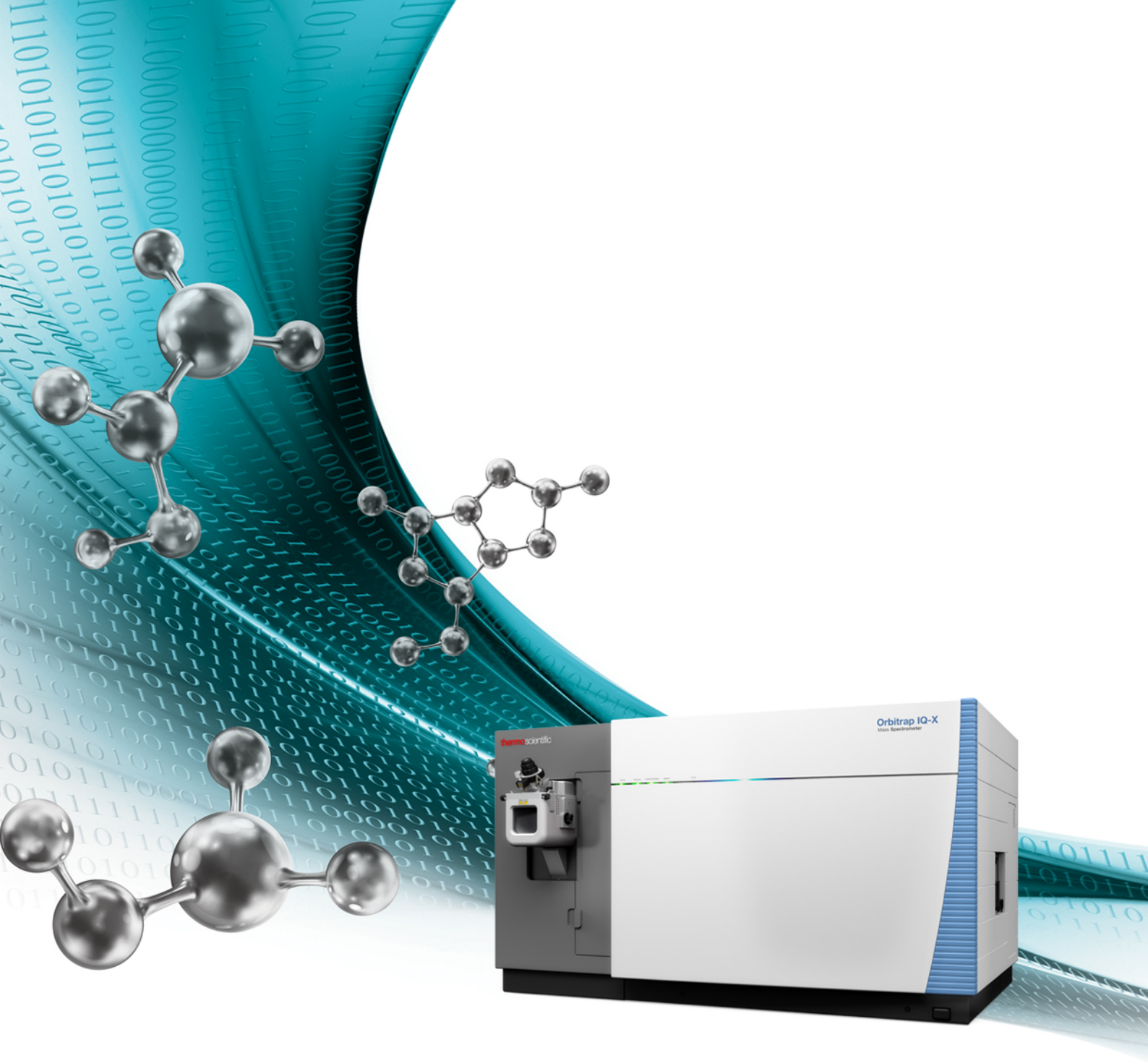

Designed to unravel complex chemical structures

Orbitrap IQ-X Tribrid mass spectrometer

Learn more

thermo scientific

Received: 15 May 2021 | Revised: 17 August 2021 | Accepted: 23 August 2021

DOI: 10.1002/mas.21745

REVIEW ARTICLE

WILEY

Gas-phase structure of polymer ions: Tying together theoretical approaches and ion mobility spectrometry

Quentin Duez[1,2] | **Sébastien Hoyas**[1,2] | **Thomas Josse**[3] | **Jérôme Cornil**[2] | **Pascal Gerbaux**[1] | **Julien De Winter**[1]

[1]Organic Synthesis and Mass Spectrometry Laboratory, Center of Innovation and Research in Materials and Polymers (CIRMAP), University of Mons, UMONS, Mons, Belgium

[2]Laboratory for Chemistry of Novel Materials, Center of Innovation and Research in Materials and Polymers (CIRMAP), University of Mons, UMONS, Mons, Belgium

[3]Materia Nova—R&D Center, Mons, Belgium

Correspondence
Julien De Winter, Laboratory of Organic Synthesis and Mass Spectrometry (S²MOs), Université de Mons, 23, Place du Parc, 7000 Mons, Belgium.
Email: Julien.dewinter@umons.ac.be

Abstract

An increasing number of studies take advantage of ion mobility spectrometry (IMS) coupled to mass spectrometry (IMS-MS) to investigate the spatial structure of gaseous ions. Synthetic polymers occupy a unique place in the field of IMS-MS. Indeed, due to their intrinsic dispersity, they offer a broad range of homologous ions with different lengths. To help rationalize experimental data, various theoretical approaches have been described. First, the study of trend lines is proposed to derive physicochemical and structural parameters. However, the evaluation of data fitting reflects the overall behavior of the ions without reflecting specific information on their conformation. Atomistic simulations constitute another approach that provide accurate information about the ion shape. The overall scope of this review is dedicated to the synergy between IMS-MS and theoretical approaches, including computational chemistry, demonstrating the essential role they play to fully understand/interpret IMS-MS data.

KEYWORDS

computational chemistry, ion mobility spectrometry, polymers

1 | INTRODUCTION

Polymers and associated polymeric materials are ubiquitous and strongly contribute to the advent and development of advanced materials in diverse areas such as automobile, textile, packaging, medicine, pharmacy, and so forth (Dubois et al., 2009). For high value applications, (high) performance materials are designed to exhibit specific properties and/or to respond to specific stimuli, that is, T°, pH, sonication, magnetism, shocks, and so forth (Wei et al., 2017). By definition, the macroscopic properties of synthetic polymers, such as toughness, visco-elasticity and crystallinity, are closely related to their chemical structure, that is, molecular weight distribution (MWD), (co-)monomeric nature, tacticity, arrangement, and so forth (Räder & Schrepp, 1998). In this regard, the precise and accurate determination of the mass parameters are of particular interest in polymer science: (i) molecular weights, namely the *number* and *weight average molecular weights* (M_n and M_w), (ii) the MWD, also defined as the *molar mass dispersity* ($Đ_M$), and (iii) the nature of the polymer itself (Räder & Schrepp, 1998). Well-established methods for mass parameters evaluation are *size exclusion chromatography* (SEC), vapor pressure and membrane osmometry, viscometry, light scattering and ultracentrifugation (Räder & Schrepp, 1998). SEC is definitively the most appreciated method due to its simplicity. This method relies on the measurement of mean hydrodynamic volume of the analytes by comparison with standards to determine the relative mass parameters (Lloyd et al., 1995). However, the measured quantities are affected by polymer-solvent

Quentin Duez and Sébastien Hoyas contributed equally to this study.

and polymer-stationary phase interactions, as well as polymer topology variability (dendrimer, linear, cyclic, catenanes, etc.), which complicates the obtention of reliable data (Tatro et al., 2002). Triple detection SEC circumvents this issue by measuring the absolute mass parameters but is still largely under-explored in routine mainly due to the complexity of the technique (Laguna et al., 2001).

Nuclear magnetic resonance (NMR) is another popular technique in the context of polymers characterization (Macha & Limbach, 2002). In particular, proton NMR provides insights about the repeating unit and end-groups chemical nature. M_n can be further derived from their signal integration ratio. Interpretation and data treatment is unavoidably complicated when different end groups are present, and because of signal overlapping over the narrow proton NMR chemical shift range (Izunobi & Higginbotham, 2011).

While NMR and SEC provide useful data on polymer structures and mass parameters, they can yield ambiguous results, especially in the case of complex topologies (cyclic, branched, etc.) and/or when high molecular weight (co-)polymers are analyzed (Gaborieau & Castignolles, 2011; Izunobi & Higginbotham, 2011).

Mass spectrometry (MS) can be considered as an ideal tool for the structure elucidation of both organic and inorganic polymers thanks to its high sensitivity and broad dynamic range (Macha & Limbach, 2002; Räder & Schrepp, 1998). MS requires the formation of gaseous ions from analyte to subsequently measure their mass-to-charge ratio (m/z) (Hanton, 2001). Although MS is now considered as an essential analytical technique for polymer characterization, it is worth to note that many years of development were needed to fully exploit its potential. Indeed, the most critical parameter revealed to be the production of intact ions in gas phase.

Initially, the polymer samples were characterized in an off-line fashion by MS analysis of their degradation products from pyrolysis (Bradt et al., 1953; Davison et al., 1954; Lehrle & Robb, 1959; Madorsky & Straus, 1948; Martin, 1959; Radell & Strutz, 1959; Völlmin et al., 1966; Wall, 1948). An important evolution regarding ionization and transfer to gas phase was the introduction of field desorption (FD) ionization in the late seventies (Schulten & Lattimer, 1984). For many years, FD was considered as the benchmark for macromolecules analysis since it was the only source able to manage the transfer of intact chains (>10,000 g/mol) to the mass analyzer(s) (Rollins et al., 1990). However, the most significative breakthrough for polymer analysis by MS occurred in the 80's when "soft" ionization sources, that are, matrix-assisted laser desorption/ionization (MALDI) and electrospray ionization (ESI) were developed almost nearly simultaneously by Tanaka et al. (1988), Karas et al. (Karas et al., 1985; Karas & Krüger, 2003) and by Yamashita and Fenn, respectively (Yamashita & Fenn, 1984). Using these ionization sources, high molecular weight ions up to 100,000 g/mol can be produced, mass-analyzed, and finally detected without any significant fragmentation (Karas & Hillenkamp, 1988; Tanaka et al., 1988).

The introduction of aforementioned "soft" ionization sources paved the way for the study of intact macromolecules, which enabled a precise determination of mass parameters and of the nature of (co-)monomer units (Hanton, 2001; Huijser et al., 2006). This breakthrough, however, is operated to the detriment of structural information such as atoms connectivity, that could be deduced through "hard" ionization sources. To cope with this limitation, multistage MS experiments including ion decomposition have been developed over the years (Barner-Kowollik et al., 2012; de Hoffmann & Stroobant, 2007) Basically, the identification of the decomposition products involves two (or more) consecutive mass analyses (de Hoffmann & Stroobant, 2007). Multistage MS analytical technique was extensively used in the context of polymer characterization over last three decades (Wesdemiotis et al., 2011). Indeed, by using this specific method, it is possible to determine the end-groups nature or even differentiate the polymer topologies, for example, cyclic versus linear structures, by analyzing the fragmentation patterns and/or comparing the energy of dissociation (Josse et al., 2015). More examples of successful multistage MS applications can be found in recent reviews (Wesdemiotis, 2017; Wesdemiotis et al., 2011).

The most recent quantum leap for polymer characterization is the introduction of ion mobility spectrometry coupled to mass spectrometry (IMS-MS) (Gidden et al., 2000; Larriba & Fernandez De La Mora, 2012; Trimpin et al., 2007; Ude et al., 2004; von Helden et al., 1995a). Although different IMS setup are commercially available, the basic principles remain similar, that is, the separation of ions depending on their size and shape. IMS experiments consist in the introduction of ions in a cell pressurized by a buffer gas (typically He or N_2) under the influence of an electric field. The ions are then separated according to their ion mobility (K), which accounts for their ease to travel through the cell. The mobility K directly depends on the charge (z) and the size of the ions (collision cross section [CCS]) (Equation 1). The CCS itself formally represents a momentum-transfer cross section, which is a temperature-dependent property of the ion-gas system that reflects their interactions (Gabelica et al., 2019; Gabelica & Marklund, 2018; Revercomb & Mason, 1975).

$$K = \frac{3ze}{16N}\sqrt{\frac{2\pi}{\mu k_B T}}\frac{1}{\mathrm{CCS}}. \quad (1)$$

In this equation, N is the buffer gas number density, T the temperature, k_B the Boltzmann constant, e the elementary charge, and μ the reduced mass of the ion-gas pair.

The possibility to separate ions based on their size and shape is widely exploited in various research field such as proteomics (Konijnenberg et al., 2013; Sinclair et al., 2018; Uetrecht et al., 2010) metabolomics (Luo et al., 2020) or glycans identification (Chen et al., 2018; M. A. Ewing et al., 2016; Pu et al., 2016). Among them, the identification of the protein ions shapes is particularly popular. Indeed, the ability to assess whether a protein is in a "native-like" or denatured state based on its shape as a gaseous ion is very appealing (Stojko et al., 2015; Veale et al., 2020). Furthermore, IMS experiments involving collision activation (collision-induced unfolding [CIU]) can be performed to probe the stability of native-like conformations (Dixit et al., 2018; Hopper & Oldham, 2009; Sun et al., 2015).

Besides the numerous publications about biological materials, IMS is increasingly employed for synthetic polymer characterization. However, the overall picture is significantly different. Indeed, proteins are monodisperse ($Đ_M = 1$) and therefore characterized by a unique composition and a distribution of charge states (Bornschein et al., 2011; Borysik et al., 2004). On the other hand, synthetic polymers occupy a particular place in the field of IMS-MS. Because of their intrinsic dispersity ($Đ_M > 1.00$), they offer a broad range of homologous ions with different lengths that can form adducts with one or several cations (Crotty et al., 2016; Montaudo et al., 2006; Weidner & Trimpin, 2010). Therefore, the evolution of IMS features throughout this distribution of self-similar ions is generally the cornerstone of polymer IMS-MS investigations (Austin et al., 2021; Crescentini et al., 2019; De Winter et al., 2011; Duez, Josse, et al., 2017; Haler et al., 2017; Hoskins et al., 2011; Kim et al., 2014; Larriba et al., 2014; Larriba & Fernandez De La Mora, 2012; Morsa et al., 2014; Tintaru et al., 2014; Trimpin & Clemmer, 2008). However, it is hardly possible to assign a conformation to an ion only based on its CCS value.

Several approaches have been developed to cope with this issue and fully interpret IMS-MS data. First, the fitting of CCS trends, that is, the evolution of the CCS of a compound with a repetitive pattern (a polymer) as a function of mass, is proposed as a way to derive structural and physicochemical properties of polymer ions. A second approach takes advantage of computational chemistry to describe the three-dimensional structures of experimentally sampled ions at the atomistic level. The scope of this review will be to describe how these two approaches have been employed so far for the characterization of polymers. This review will strive to shed a light on significant advances achieved for the structural characterization of polymer ions with the strong and inextricable support of theoretical approaches.

IMS-MS has also been successfully applied as an stand-alone analytical tool to separate isomeric polymers with different topologies (Alexander et al., 2018; Foley et al., 2015; Hoskins et al., 2011; Liénard et al., 2020; Mao et al., 2019), complex polymer blends (Barrère et al., 2014; Snyder & Wesdemiotis, 2021; Trimpin et al., 2007; Trimpin & Clemmer, 2008), or copolymers (Amalian et al., 2019; Baker et al., 2004; Duez, Moins, et al., 2020; Ito et al., 2019; Jackson et al., 2004). While these topic will not be discussed in this review, we refer the readers to a recent review with a broader scope about polymer analysis with IMS-MS (Charles et al., 2020).

It should be noted that the following discussion distinguishes synthetic polymers (simply referred as polymers) and peptides. Peptide IMS-MS literature does not always refer to polymer data for several reasons. Most polymer IMS-MS reports deal with polyethers and polyesters that are straightforward to analyze and easily ionizable as they form adducts with alkali ions (Li^+, Na^+, K^+, etc.) by charge-dipole interactions. Additionally, these polymers often behave as random coils in solution (Alessi et al., 2005; Tonelli, 2014), unlike peptides which can form highly organized structures that are stabilized by a network of strong intramolecular interactions (Hudgins & Jarrold, 1999; Jas & Kuczera, 2004; Kohtani et al., 2004; Wang et al., 2006). Total or partial retention of solution-phase conformations upon ionization and transfer into the gas phase is thus not expected for most floppy polymers, in contrast to peptides (Hudgins et al., 1999; Hudgins & Jarrold, 1999). As outlined in the next paragraphs, this implies that the gas-phase structures of polymer ions are only governed by their ability to fold around and to screen the complexed charge(s).

2 | TREND LINE ANALYSIS

As discussed above, the MS analysis of a polymer sample directly reflects its chain length dispersity. When coupled to IMS, the arrival time distribution of each ion is recorded, which results in a wide distribution of CCS over all detected chain lengths and charge states. A unique feature of polymer analysis by IMS-MS consists in the monitoring of IMS data evolution for a given charge state either as a function of mass (or m/z), as a function of the number of repeating units (degree of polymerization

[DP]), or as a function of the atom number. This enables the detection of subtle modifications in the gas-phase structure of macroions. For instance, it allows to separate macroions of different topologies, such as cyclic and linear polymers, or shape changes due to ionization by protonation or complexation of alkali/metal ions (Duez, van Huizen, et al., 2019; Haler et al., 2020; Hoskins et al., 2011; Kim et al., 2014; Liénard et al., 2020; Morsa et al., 2014; Tintaru et al., 2014; Trimpin et al., 2007; Trimpin & Clemmer, 2008). Ultimately, the mathematical fitting of CCS "trend lines" enables to derive quantitative data relevant to the investigated polymer, as discussed below (Duez, Liénard, et al., 2019; Frerichs et al., 2021; Haler et al., 2018; Kokubo & Vana, 2017; Ruotolo et al., 2008; Saintmont et al., 2020). This data fitting provides the contribution of each monomer unit to the global CCS (Figure 1).

In 2008, Ruotolo et al. proposed the following equation to fit the CCS of globular protein complexes as a function of their mass M:

$$CCS = A.\ M^{2/3}, \tag{2}$$

with A being a fitting parameter directly related to the ion density. This equation was proposed since it accounts for the surface evolution of a growing sphere. Indeed, for a sphere with a radius R, a mass M and a density ρ, the collision cross section CCS is proportional to $M^{2/3.}$ The sphere volume can also be approximated by the product of the number of monomer unit with the mean volume of the unit in gas phase (Haler et al., 2018), as demonstrated below:

$$CCS = \pi R^2 \quad \text{and} \quad V = \frac{4\pi R^3}{3} = \frac{M}{\rho}. \tag{3}$$

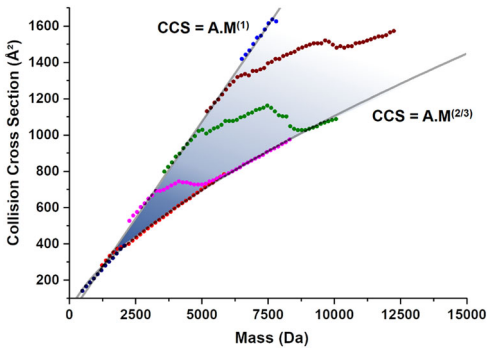

FIGURE 1 Fitting of CCS "trend lines" for polylactide ions with charge $z = 1+$ to $6+$. Two trend lines $CCS = A.\ M^{2/3}$ and $CCS = A.\ M^{1}$ are shown [Color figure can be viewed at wileyonlinelibrary.com]

$$R = \sqrt[3]{\frac{3M}{4\pi\rho}}. \tag{4}$$

$$CCS = \left(\frac{3\sqrt{\pi}}{4\rho}\right)^{2/3} M^{2/3} = A \quad M^{2/3}. \tag{5}$$

Equation (5) has been used to evaluate the gas-phase density of protein assemblies and dendrimers (Marklund et al., 2015; Saintmont et al., 2020). Since the mass M of a polymer ion is directly proportional to the number of repeating units, M and DP are interchangeable in Equation (5).

In the field of synthetic polymers, Kokubo and Vana were the first to take advantage of IMS-MS data fitting to determine targeted physico-chemical properties. In a first approach, they derived the characteristic ratio C_n, that accounts for chain stiffness, of poly(ethylene glycol) (PEG) and poly(propylene glycol) (PPG) (Kokubo & Vana, 2016). Their model was based on the fitting of CCS/DP data of spherical objects without any perturbation of the complexed charge. Consequently, only globular or nearly globular ions should be considered. To this end, they restricted the analysis to singly charged PEG and PPG ions. The C_n values derived from IMS measurements are remarkably close to literature values obtained using solution-phase characterization methods, such as viscosity measurements (Allen et al., 1967; Beech & Booth, 1969; Kokubo & Vana, 2016; Sasanuma, 1995). This approach was then used to probe the influence of the sequence of triblock copolymers on their C_n values (Frerichs et al., 2021).

They later went a step further by evaluating the dielectric constant of polymers from the gas-phase behavior of doubly charged PEGs. Doubly charged polymer ions can adopt either extended or globular gas-phase structures depending on their charge screening efficiency (see discussion in Section 3). Briefly, larger chains will fold into spherical objects while shorter macroions will adopt extended shapes due to the electrostatic repulsion between charges. The breaking point between these two regimes, also called "structural transition," is characterized by an inflection point in CCS/DP evolutions (De Winter et al., 2011; Larriba & Fernandez De La Mora, 2012; Trimpin & Clemmer, 2008; Ude et al., 2004). By assuming a balance between repulsive electrostatic and retracting entropic forces, Kokubo and Vana estimated the relative dielectric constant of PEG based on the fitting of CCS trends. The obtained value (7.22) was lower than reported literature values measured in bulk with 1% water contamination (8.95–10.95). This divergence was attributed to the measurement of the dielectric constant for naked ions in the gas phase, rather than in bulk with water contamination.

In 2018, Haler et al. (2018) proposed an IMS data fitting method to derive structural interpretations for polymer ions without any additional input or a priori from computational chemistry. In a first approach, they fitted CCS evolution of linear poly(ethoxyphosphate) (PEtP) chains with charge states varying from 1+ to 8+ with the following equation:

$$CCS = A.\ DP^B, \tag{6}$$

where A and B are fitting parameters. For each fitting, B values were always close to 2/3 while A was varying between 65 and 90. Note that their fitting approach was here not only restricted to globular polymer ions, but rather to larger CCS data sets comprising many different charge states, chain lengths, and hence disparate gas-phase structures. They attributed variations of the A parameter to changes in the "apparent density" of macroions, which can be directly related to their gas-phase structure. Indeed, highly charged polymer ions will adopt extended conformations due to charge-induced instabilities (De Winter et al., 2011; Larriba & Fernandez De La Mora, 2012; Trimpin et al., 2007; Ude et al., 2004), thereby resulting in lower 'apparent densities'. In a second approach, they constrained the parameter B to 2/3 and analyzed ratios of A for consecutive CCS trends. By doing so, Haler et al. (2018) were able to predict chain lengths at which structural transitions between extended and compact ion shapes are expected. They later applied their approach to interpret charge solvation effects for polymers with different backbone natures. For instance, by comparing two polyoxazolines with different side chains and monomer sizes, they evidenced that the contribution of the chain flexibility was directly reflected in the A parameter (Haler et al., 2021).

The approach proposed by Haler et al. considers fitting of CCS as a function of DP, which might lead to ambiguous results when comparing polymers with different monomer sizes and different end-groups. Indeed, DP only stands for the number of repeating units without considering chain ends, that might also take part in charge solvation and have a critical impact on the measured CCS. Building on this approach, our group investigated the fitting of IMS data for globular PEG and poly(L-lactide) ions with a wide variety of chain ends (Duez, Liénard, et al., 2019). In a first approach, we performed CCS/DP fittings with the following model:

$$CCS = A.\ DP^B + End, \tag{7}$$

where End, A and B are fitting parameters, the latter being fixed at 0.66 since only globular ions were considered. In this equation, the contribution of the chain ends, that is, when DP = 0, is encompassed in End. The nature of the end group was found to significantly impact both A and End parameters, making the cross-comparison of different polymers difficult to interpret (Figure 2A,B). We thus proposed to account for both the end groups and repeating units by fitting CCS datasets according to atom number. By doing so, the cross-comparison of CCS trend lines becomes possible for any polymer with any end-groups. Especially, it enables to characterize polyesters made of isomeric backbones and bearing different end-chain groups (Duez, Liénard, et al., 2019).

Finally, the relevance of CCS trends fitting for non-globular ions can be argued. Indeed, only the fitting of the CCS for spherical ions is supported by mathematical models. For other ions, that is, when B deviates from 2/3 (Equation 6), care should be taken for data interpretation. It was recently shown that B critically depends on the range of data available for fitting for nonglobular ions (Hoyas et al., 2020). Peptoids compounds that belong to the polyamides family may adopt nonglobular conformations, such as helices (that can be approximated by a cylinder of growing height). Model peptides and peptoid helices were investigated by molecular modeling. Theoretical CCS/mass evolutions were fitted as a function of mass (instead DP) by Equation (6) (Figure 2C). The impact of the available data range for fitting was highlighted by several fittings with increasing upper limits of the mass range (500 Da < upper limit < 10,000 Da). For a given upper limit, the B parameter is always higher than 2/3 but not equal to 1 as it would be expected for perfectly cylindrical objects. B rather evolves towards 1 as the range of available data increases (Figure 2D). Therefore, fitting parameters for nonglobular ions can be misleading as they critically depend on the mass range under consideration (Hoyas et al., 2020).

Altogether, while fitting of IMS data provides a rapid screening over large datasets (Haler et al., 2020; Marklund et al., 2015; Ruotolo et al., 2008) and enables to derive quantitative physicochemical data for globular ions (Duez, Liénard, et al., 2019; Kokubo & Vana, 2016, 2017; Saintmont et al., 2020) it fails to provide unambiguous structural information at the atomistic level since it only highlights differences between globular ($B = 2/3$) and nonglobular ions ($B \neq 2/3$). Hence, interpretation of IMS data fittings should always be supported by adequate theoretical simulations to assess the conformations adopted by polymer ions in gas phase.

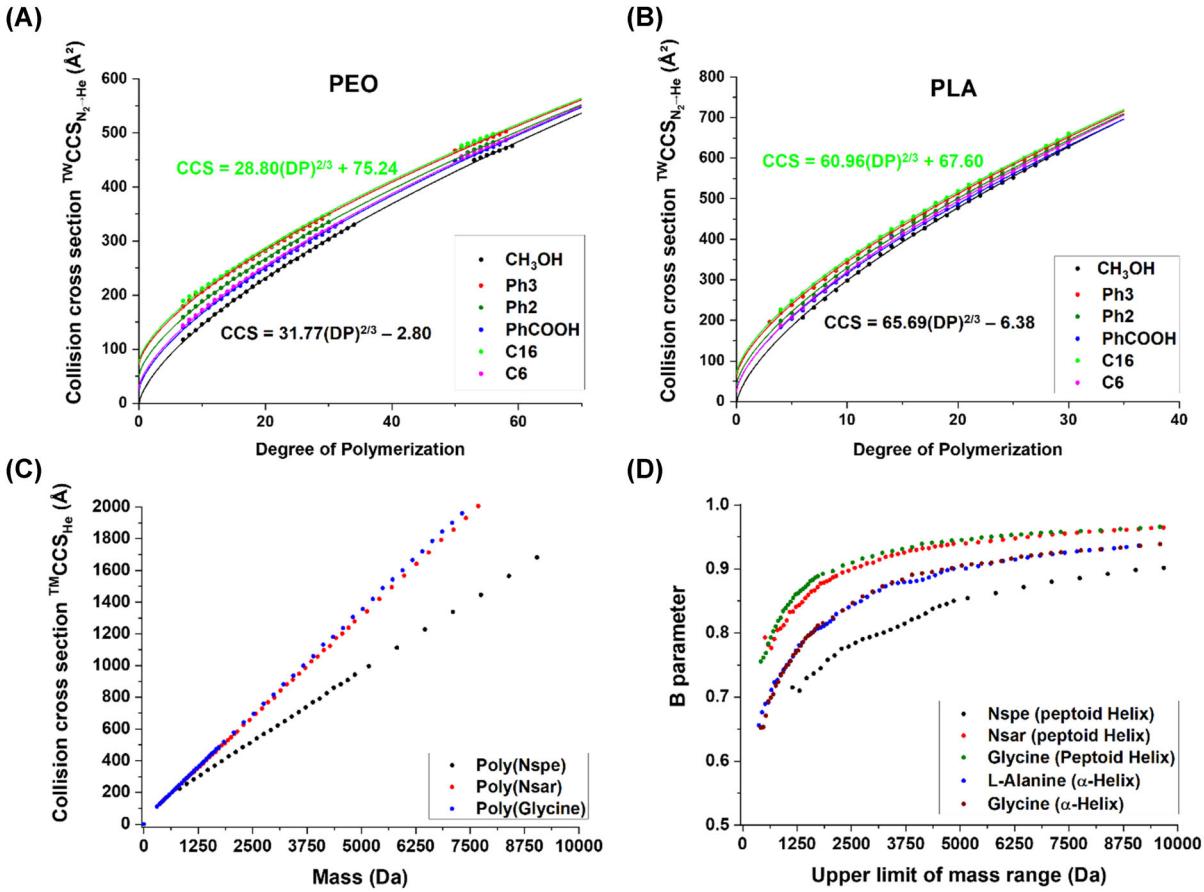

FIGURE 2 (A,B) Experimental CCS trend lines ($CCS = A.\ DP^{2/3} + End$) for globular α-methyl ω-hydroxy and α-methyl ω-ester-PEO and PLA ions functionalized with various chain ends. Adapted from reference (Duez, Liénard, et al., 2019). (C) Theoretical CCS trend lines ($CCS = A.\ M^B$) as a function of mass for ideal peptoid helices. (D) Evolution of the B parameter with the mass range for ideal peptoids and peptides helices, as obtained by fitting of theoretical CCS trend lines. Adapted with permission from reference (Hoyas et al., 2020). Copyright 2020 American Chemical Society. CCS, collision cross section; PLA, poly(L-lactide) [Color figure can be viewed at wileyonlinelibrary.com]

3 | PREDICTION AND INTERPRETATION OF CCSs BASED ON ATOMISTIC SIMULATIONS

The development of atomistic simulations has sparked a particular interest in the field of IMS-MS since it enables the study of (i) ion conformations; (ii) conformational dynamics; and (iii) strength of intramolecular interactions involved in the stabilization of gas-phase structures. In addition, the simulation of gaseous ions is appealing because solvent effects are not considered. To link experimentally sampled structures and modeled conformations, three steps must be followed: (i) the generation of candidate conformations, (ii) the calculation of their theoretical CCS, and (iii) the confrontation of experimental and theoretical data. The first two steps are strongly conditioned by the system under consideration (Figure 3). Indeed, different levels of complexity/precision must be considered depending on the size and nature of the modelled compound. In this section, we will first cover reported methods to compute theoretical CCS and then discuss ways to generate the candidate geometries, depending on the size and nature of the system under study. Finally, concrete examples of the coupling between IMS and modeling for synthetic polymer analysis will be outlined.

3.1 | CCS calculation

As described above, the CCS represents a momentum-transfer cross section, a temperature-dependent property of the ion-gas system that reflects interactions between ions and gas molecules (atoms). This interaction can be handled in different ways. As a first approach, ions and gas molecules can be considered as hard spheres assemblies undergoing elastic scattering. More elaborate and computationally expensive methods are also developed to consider complex collision events and long-range interactions.

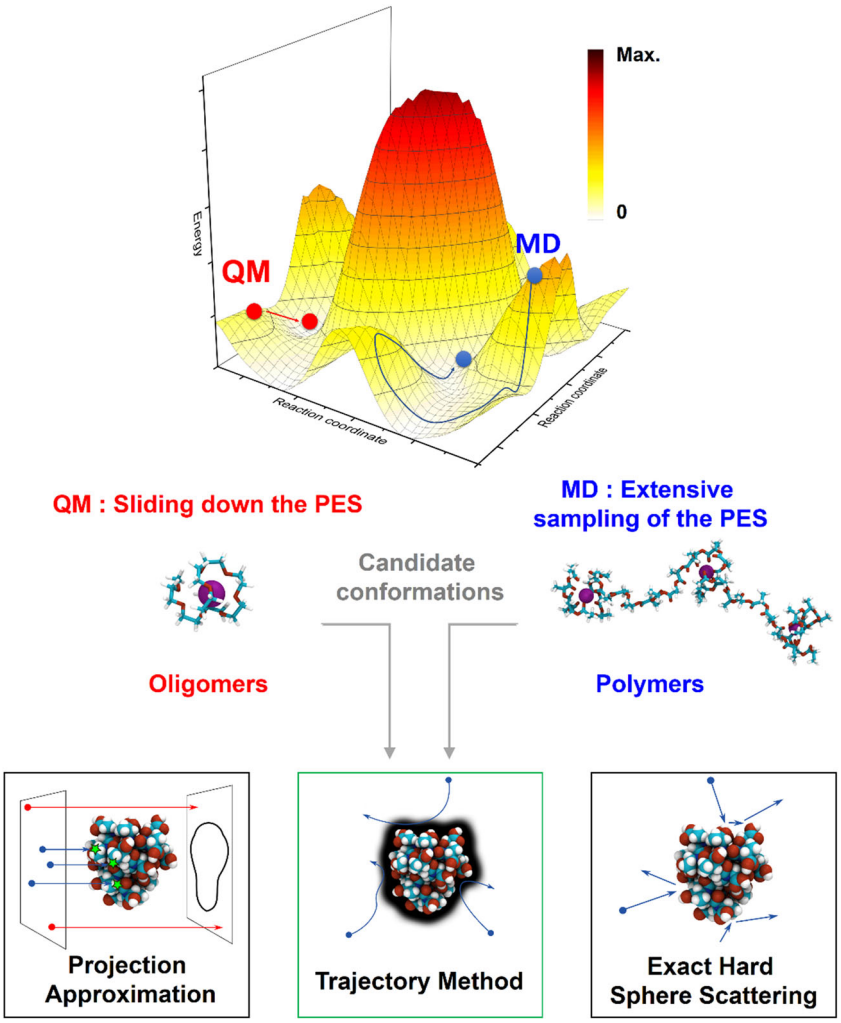

FIGURE 3 General workflow for interpretation of IMS-MS data with atomistic simulations. Top. Schematic representation of the PES of a polymer ion. Red areas correspond to unfavorable high energy conformations while white spaces represent energy minima. Bottom. Generation of candidate conformations by QM or by classical MD methods. The obtained conformations are then submitted to collision cross section calculations with the projection approximation, exact hard sphere scattering and trajectory methods algorithms. Adapted from reference (Prell, 2019). MD, molecular dynamics; PES, potential energy surface; QM, quantum mechanical [Color figure can be viewed at wileyonlinelibrary.com]

3.1.1 | Projection approximation (PA)

The simplest, fastest, and most widely spread method to compute CCS_{th} is the "Projection Approximation" (Marklund et al., 2015; Mesleh et al., 1996; Paizs, 2015; Rayleigh, 1882). This algorithm, based on the work of Mack, approaches the three-dimensional structure of a system as a two-dimensional quantity by only considering its projected shadow area. Each atom of the system is represented by a hard-sphere whose radius r_i is typically close to their van der Waals radius (von Helden et al., 1993). A first projection orientation is randomly selected, and the shadow of all atoms is projected on a surface, enclosed by a box of known area. Several thousands of spots, whose radius r_g depends on the collision gas, typically helium, are randomly defined on the plane of projection. A "hit" (1) is counted when a spot is located within a radius $r \leq (r_i + r_g)$. Otherwise, spots are treated as "misses" (0). The fraction of "hits" is then computed and multiplied by the area of the box, resulting in the value of the projected area of the system in the first orientation. The same procedure is repeated for several thousands of random orientations and the averaged value corresponds to the rotationally averaged CCS, ^{PA}CCS (Prell, 2019). The PA is the most computationally inexpensive CCS algorithm. Indeed, only a few minutes are required to compute the ^{PA}CCS for the Norwalk virus capsid (PDB code 1IHM ~170 kDa) (Bleiholder et al., 2011; Marklund et al., 2015; Paizs, 2015). However, the PA suffers from several drawbacks. First, since the system is represented by hard spheres without external potential, temperature effects are not considered. In addition, surface roughness is also neglected, which can dramatically impact the CCS. Indeed, complex collision processes, such as multiple scattering or grazing scattering, can occur but are not accounted for in PA (Gabelica & Marklund, 2018; Larriba & Hogan, 2013; Mesleh et al., 1996; Prell, 2019). Finally, since the PA only accounts for a shadow projection, cavities are ignored. The PA will thus return the same result for a "hollow" and a "solid" ion. This algorithm may therefore not be suitable for polymers that may form pockets, like dendrimers (Bleiholder et al., 2011;

Memboeuf et al., 2011; Saintmont et al., 2020). Because of this shortcomings, the computed ^{PA}CCS is often underestimated compared to experiments and to the reference method for the theoretical CCS calculation (see Section 3.1.3). As a result, ^{PA}CCS deviate by about 7% compared to experimental values for small ions (<100 Å^2) and up to 20% for complex protein shapes (Bleiholder et al., 2011; J. W. Lee et al., 2017).

Since the first implementation of the PA in MOBCAL (Mesleh et al., 1996; von Helden et al., 1993), improved PA-based algorithms have been developed, such as the Projected Surface Approximation (PSA) and the Local Collisional Probability Approximation (LCPA) (Anderson et al., 2012; Bleiholder, 2015; Bleiholder et al., 2011; Bleiholder, Contreras, & Bowers, 2013; Bleiholder, Contreras, Do, et al., 2013). These algorithms better consider surface roughness and concavity through the use of a shape factor. PSA results nicely agree with the computationally expensive Trajectory Method (TM; see below), typically within 5% (Bleiholder et al., 2011), but is only available as a web service on which a limited number of input structures can be analyzed (*Projected Superposition Approximation Webserver*, n.d.).

The low computational cost of the PA and related algorithms makes them generally more suitable for very large systems that cannot afford more computationally expensive methods, typically proteins or virus capsids weighing several hundred thousand Da (Jurneczko & Barran, 2011; Marklund et al., 2015; Pukala et al., 2009). In addition, optimized parametrization and/or domain decomposition approaches are developed to further reduce computation time (Marklund, 2015; Marklund et al., 2015; Paizs, 2015).

3.1.2 | Exact hard-sphere scattering (EHSS)

The EHSS algorithm was first introduced by Shvartsburg and Jarrold (1996). Unlike the PA algorithm, EHSS considers a three-dimensional approach in which polyatomic ions are represented by hard spheres whose radii depend on actual van der Waals radii. The algorithm determines whether a gas particle with a known direction and impact parameter collides with one of the hard spheres constituting the ion, and into which direction the particle will scatter after the impact. After collision, the direction and the impact parameter are updated, and the algorithm determines whether a new collision is possible. In this case, the process is repeated until no further collisions are achievable (Prell, 2019; Shvartsburg & Jarrold, 1996). Several thousands of collisions are simulated and the final scattering angles relative to the initial incoming directions are recorded for each initial orientation to compute the CCS. Since its original implementation in MOBCAL (Mesleh et al., 1996), an improved EHSS algorithm, EHSSRot, has been proposed. This approach introduces rotation of the ion during the scattering process, thereby providing more accurate results (Shvartsburg et al., 2007). The advantage of EHSS over P(S)A/LCPA is the explicit consideration of the ion surface and of multiple scattering events.

The impact of multiple collision events was especially highlighted for the computation of ^{EHSS}CCS for the Norwalk virus capsid (Bleiholder et al., 2011). Indeed, by modifying the EHSS algorithm to only consider single collision events (EHSS-SC), Bleiholder et al. found that their $^{EHSS\text{-}SC}$CCS is systematically underestimated compared to experimental CCS values, alike the PA, which demonstrates the importance of multiple collision events. However, ^{EHSS}CCS generally deviate from experiments by more than 10% for small ions (<100 Å^2). Other modified versions of EHSS called "Diffuse Hard Sphere Scattering" and "Trajectory Diffuse Hard Sphere Scattering" were shown to improve the accuracy for large cluster ions (Larriba & Hogan, 2013; Shrivastav et al., 2017). In these algorithms, scattering events are considered to be diffusive rather than strictly specular to account for the rotational and vibrational energy. The EHSS algorithm (and variants) are available in several softwares (MOBCAL (Mesleh et al., 1996; Shvartsburg & Jarrold, 1996), IMoS (Larriba & Hogan, 2013; Shrivastav et al., 2017), EHSSRot (Shvartsburg et al., 2007), and IMPACT (Marklund et al., 2015)). Overall, EHSS methods provide satisfactory results with low computational cost for a large range of systems including native-like ions of a tens of kDa (J. W. Lee et al., 2017). However, since they do not consider long-range interactions, temperature effects are not reproduced. This drawback is ruled out with the TM approach.

3.1.3 | Trajectory method

The TM was first reported by Mesleh et al. (1996). Alike EHSS, TM simulates collisions between gas particles and the ion of interest and considers multiple scatterings. The main difference with EHSS is that TM computes a realistic potential around the ion. This accounts for long-range interactions, thereby enabling the description of temperature and charge effects. Moreover, size and shape effects are intrinsically included in this model. In their initial report, Mesleh et al. (1996) described their potential by a two-part expression composed of a 6–12 Lennard-Jones interaction and a charge-induced dipole interaction. Since helium was used in experiments for the initial report, all parameters were optimized to compute

CCS in this gas. With the advent of commercial TWIMS instruments operating in N_2, optimized Lennard-Jones parameters were reported for computing ^{TM}CCS in N_2 (Campuzano et al., 2012). TM is currently referred as the "gold standard" method for the obtention of theoretical CCS because results are very accurate (typically within 5% of experimental values (Zanotto et al., 2018), although smaller errors can be achieved by tuning the long-range potential parameters (J. W. Lee et al., 2017)) for a large variety of compounds (organic clusters, small proteins, polymers) (Bleiholder et al., 2011; De Winter et al., 2011; Lanucara et al., 2014), even with highly complex topologies (J. W. Lee et al., 2017). Moreover, the previously described algorithm families, PA and EHSS, are always compared to the TM to assess the quality of the results (Bleiholder et al., 2011; Lanucara et al., 2014; J. W. Lee et al., 2017; Marklund et al., 2015). However, the TM algorithm is computationally expensive and is thus avoided for large systems. For instance, a ^{TM}CCS computation for the Norwalk virus capsid requires more than a month of computational time with MOBCAL's original TM implementation. As mentioned above, a ^{PA}CCS computation on the same system only lasts for several minutes (Bleiholder et al., 2011). Since then, other CCS computation algorithms based on TM were developed to improve the performance of MOBCAL, that was also updated recently to improve the computational efficiency. For instance, parallelized algorithms like Collidoscope (S. A. Ewing et al., 2017), CoSIMS (Myers et al., 2019), and MobCal-MPI (Ieritano et al., 2019) were found to dramatically improve the performances of the original MOBCAL. TM has been proven to be very well suited for the study of synthetic polymers and provides results very close to the experimental values (Anderson et al., 2005; De Winter et al., 2011; Duez, Metwally, et al., 2020; Duez, Moins, et al., 2020; Haler et al., 2020). The TM algorithm is available in multiple softwares, including MOBCAL (Ieritano et al., 2019; Mesleh et al., 1996), IMoS (Larriba & Hogan, 2013; Shrivastav et al., 2017), Collidoscope (S. A. Ewing et al., 2017), CoSIMS (Myers et al., 2019), and HPCCS (Zanotto et al., 2018).

3.2 | Generation of candidate conformations: Atomistic simulations

Before the CCS calculation, a set of candidate geometries must be generated. Unlike CCS calculation algorithms, there are no "gold standard" methods. In the field of proteins, candidate geometries can be generated from X ray diffraction or NMR experiments (Anderson et al., 2012; Prell, 2019). However, since synthetic polymers are constituted of a distribution of macromolecules, solution-phase measurements cannot provide candidate geometries for individual chains. Therefore, candidate geometries must be built "from scratch" (Prell, 2019). However, after generation, the initial system is likely trapped in a local minimum on its potential energy surface (PES). The PES has thus to be scanned to produce candidate geometries and approach the experimentally sampled conformations. Depending on the size and nature of the system, several methods can be used with different levels of precision. These methods will be shortly described in the next paragraphs.

3.2.1 | Quantum mechanical (QM) methods

QM methods are generally very accurate to describe the PES since electrons are treated explicitly. The PES is sampled by modifying the initial geometry, that is, by changing the orientation of rotatable bonds and then perform a geometry optimization to find a new local or global minimum. QM methods typically include Hartree-Fock, Coupled Cluster or Density Functional Theory (DFT), although the latter is generally considered as an independent approach (see below). These methods are mainly limited to small molecular systems with only a few rotatable bonds (<150 atoms) due to their high computational cost (Lapthorn et al., 2013). Hence, for conformational studies on polymer ions, QM methods are often restricted to the study of oligomers and are unpractical for the investigation of full-grown polymers. The few QM studies on polymers were performed with DFT. Compared to other QM methods, DFT treats electrons explicitly by describing them as a systemwide electron density, resulting in a lower computational cost (Johansson et al., 2013). Nonetheless, DFT generally lacks the description of dispersion interactions (Craig et al., 2020), that is, the attractive interactions at short range that can be relevant for the folding of polymer chains. Fortunately, a dispersion correction can be applied and is very computationally effective. Consequently, DFT is one of the most popular QM methods for polymers, as it enables the study of larger oligomers with sufficient accuracy. However, achieving good accuracy requires the choice of a proper functional to correctly describe the system under consideration and thus often involves benchmarking (Memboeuf et al., 2011; Van Mourik et al., 2014).

Among the few DFT studies on the structure of gaseous oligomers, Memboeuf et al. (2011) investigated the impact of the cation on the coordination sphere of singly charged PEG oligomers (up to 18 units; ~130 atoms). They found that the structure of cationized PEG

oligomers is determined by the packing of the chain around the charge. Indeed, alkali cationizing agents (Li^+, Na^+, K^+, and Cs^+) dramatically affect the polymer packing because of their different coordination shells formed by charge-dipole interactions with the backbone oxygens. Their computations predict that coordination numbers vary from about 5 for Li^+ to 11 for Cs^+. Interestingly, they found that the gas-phase structure of PEG ions is not significantly affected by the nature of the bound cation, except for Cs^+ complexes that are significantly larger than their Li^+, Na^+, K^+ counterparts.

While QM methods are rarely used to describe the conformation of polymer ions, they are sometimes employed to derive force field parameters for classical methods (see below). It can be envisioned that future works on gaseous polymer ions will take advantage of semi-empirical methods to reduce computational cost of QM methods. Semiempirical approaches treat only the valence electrons explicitly while the core electrons are approximated by empirical parameters (Bannwarth et al., 2021; Porrini et al., 2017). These methods have already been used to describe systems whose size is up to thousands of atoms. In addition, they were already employed to describe the formation of hydrogen bonds in nucleic acids, in conjunction with IMS experiments (Porrini et al., 2017). However, empirical parameters may not always be properly defined for the systems under investigation.

3.2.2 | Classical methods

As introduced above, polymers occupy a unique place in the field of IMS-MS due to their intrinsic dispersity. Indeed, most IMS studies of polymers take advantage of the distribution of homologous chains formed during the synthesis. For instance, the CCS evolutions of polymer ions of given charge states can be evaluated to probe shape changes with growing size (De Winter et al., 2011; Duez, Chirot, et al., 2017; Gidden et al., 2000, 2002; Haler et al., 2020, 2018; Larriba & Fernandez De La Mora, 2012). Because of the need to simulate a large range of polymer chains with various sizes, QM methods cannot be envisioned as a viable tool. In addition, with growing number of rotatable bonds, the sampling of the PES can reveal tricky and other approaches than geometry optimization must be considered. With this regard, classical simulations at the molecular mechanics (MM) and molecular dynamics (MD) levels come very handy. Within these approaches, atoms are considered as charged balls linked by springs and electrons are treated implicitly by considering partial charges (often derived from accurate QM calculations on model systems) on each atom. This approach is simplistic but has proved to be as accurate as QM for selected systems. However, electronic-dependent features such as prediction of chemical reactions cannot be explored with classical approaches (Atkins & Friedman, 2011; Leach, 2001). The PES is described by a force field, that is, a mathematical expression that directly relates atomic coordinates to potential energies. Many force fields are currently available to describe various type of compounds, such as proteins, nucleotides, small molecules, polymers and are parameterized either against experiments or high-accuracy QM calculations of model compounds.

AMBER (Gidden et al., 2002; Gidden, Jackson, et al., 1999; Gidden, Wyttenbach, et al., 1999; Jackson et al., 2004; Morsa et al., 2014; von Helden et al., 1995a), CHARMM (Duez et al., 2018; Kim et al., 2014), DREIDING (De Winter et al., 2011; Duez, Metwally, et al., 2020; Duez, Moins, et al., 2020; Hoyas et al., 2020; Mayo et al., 1990), UFF (De Winter et al., 2011), MM2 (Kokubo & Vana, 2016, 2017), constitute a nonexhaustive list of the force fields used to study polymer ions in gas phase. Most of these force fields are developed to study compounds in solution rather than in gas phase. Consequently, the accuracy of these force fields for gas-phase simulations can be questioned. Nevertheless, they provide satisfactory results to address most of the in-vacuo behavior, as recently shown by J. H. Lee et al. (2019) for gaseous proteins.

Since force fields are developed on the basis of a given set of reference compounds, they are sometimes refined by practitioners to better reproduce experimental data (Broch et al., 2017; Lemaur et al., 2013; Mottin et al., 2017; Tonnelé et al., 2019; Weiser & Santiso, 2019). In this context, some force fields are being derived from generic force fields, to adequately describe the gas-phase conformational space of polymer ions. For instance, our group reported the parametrization of the DREIDING force field against QM calculations to describe the gas-phase behavior of polyesters, namely poly(L-lactide) (PLA), and poly(propiolactone) (PPL) (Duez, Metwally, et al., 2020; Duez, Moins, et al., 2020) but also of other original polymeric compounds such as peptoids (Hoyas et al., 2018). However, the parametrization of gas-phase force fields is still scarcely explored and it is hoped that more approaches will be developed in the future, especially with the development of instruments that enable the evaluation of spectroscopic data in gas phase, such as infrared and circular dichroism (Daly et al., 2020; Jašík et al., 2013; Martens et al., 2012). These experimental data could help to refine future force field parameters for the description of gas-phase ions.

Since synthetic polymers are composed of many rotatable bonds, an extensive sampling of the PES must be

performed to obtain low-energy candidate structures. This sampling can be performed by MD or Monte Carlo (MC) simulations. MD is based on the resolution of Newton's equations to describe the time-dependent dynamics of the compound under interest. The system is typically coupled to a thermostat that provides the required energy to overcome potential energy barriers and hence to efficiently sample the PES. MD being a deterministic method, it allows to probe properties that vary in time, such as conformational rearrangement. MC, which is a stochastic method, allows to randomly explore the entire PES but it cannot provide information about time-dependent properties. Both methods are equally valid, but MD is generally preferred as it enables to study the dynamics of the system. Within the frame of MD simulations, several enhanced sampling approaches can be used, among which can be found the simulated annealing dynamics (SA) (Gidden et al., 2002; Jackson et al., 2004; von Helden et al., 1995b) and (quenched) dynamics (QD). The main difference between these two methods stands in the temperature evolution during the simulation. For SA, the temperature of the system is increased steadily while QD directly thermalizes the system to move along the PES and overcome barriers (De Winter et al., 2011; Duez, Josse, et al., 2017; Larriba & Fernandez De La Mora, 2012; Morsa et al., 2014). Over the course of the sampling, geometries are extracted and optimized at regular intervals to slide down the PES and obtain the low-lying conformers from different basins.

After sampling of the PES and identification of low-lying energy conformers, MD simulations can be performed on the most stable one. From these simulations, time-dependent properties will be computed, in particular the CCSs. A valid and common approach to compare experimental CCS to the MD results consists in extracting a few hundreds of geometries from the production MD and submit them individually to one of the CCS algorithms discussed above, typically the TM. Generally, the averaged CCS of the entire set of candidate geometries is compared to experimental CCS data (De Winter et al., 2011; Duez, Moins, et al., 2020; Haler et al., 2020; Hoyas et al., 2020; Morsa et al., 2014). However, it is also good practice to analyze the time-evolution of the CCS or the CCS distribution (Duez, Moins, et al., 2020) to potentially spot any conformational rearrangements that would lead to distinct conformations along the MD.

Due to the cheap cost of MD simulations and the continuous improvement of informatic hardware, the length of MD simulations can be extended up to several microseconds (Duez, Metwally, et al., 2020). MD simulations also enable the analysis of factors responsible for structural rearrangements, such as a dihedral switch, the proximity of charges, and so forth. Finally, the impact of the temperature on the ion can also be probed by MD, which provide qualitative insights into the polymer ion flexibility (von Helden et al., 1995b). However, there are currently no evidence that the thermostat temperature is correlated to the temperature during the experiments.

In the next sections, we will highlight how joint IMS/MD approaches have been exploited to decipher the gas-phase structure and dynamics of polymer ions.

3.3 | Gas-phase simulations

3.3.1 | Singly charged oligomers

The first IMS-MS reports on polymers were published in 1995 by the group of Bowers using a MALDI-DTIMS instrument, which mainly produces singly charged ions (von Helden et al., 1995b). These seminal studies focused on the structure of small singly charged oligomers. For instance, von Helden et al. (1995a) reported the behavior of PEG oligomers cationized with a Na^+. For each detected ion (Figure 4A), a symmetric unimodal ATD was recorded and assigned to either a single stable conformer or to rapidly interconverting isomers (von Helden et al., 1995b). To assess the conformation of these singly charged oligomers, MD simulations were performed. The agreement between experimentally and theoretically derived K_0^{-1} was excellent (Figure 4C), indicating that the recorded ATDs could be assigned to single conformers. For each modeled chain, the simulations revealed that the oxygen atoms of the most stable conformers organize around the sodium cation by charge-dipole interactions. The backbone arranges in a loop-like fashion, thereby leading to a globular structure for longer chains. As pictured in Figure 4B, up to seven oxygen atoms were found to interact with Na^+. As a comparison, a neutral PEG_9 was also modeled and its computed mobility was found to be lower than for cationized PEG_9, indicating a looser conformation. The sodium cation induces therefore a compaction of the chain when the polymer backbone folds around the charge (von Helden et al., 1995b). Complexation with other cations such as Li^+ or Cs^+ yielded similar results; Li^+ coordinates seven oxygen atoms while Cs^+ coordinates 10–11 oxygens, which is consistent with the results from Memboeuf et al. (Memboeuf et al., 2011; Wyttenbach et al., 1997).

The ability of the polymer backbone to fold around the complexed charge depends on its flexibility. To assess the role of flexibility on "charge solvation," IMS-MS analyses were performed on three polyethers, namely PEG, PPG and poly(tetramethyl ether glycol) (PTMEG), also called poly(tetrahydrofuran). From MD-generated

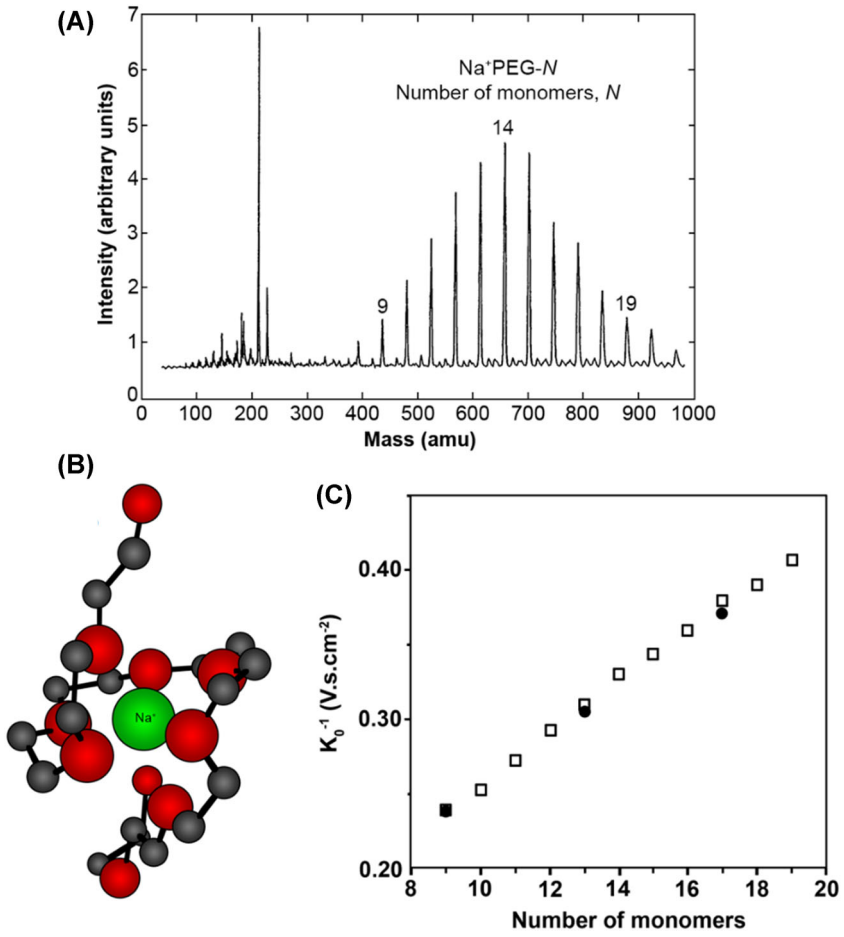

FIGURE 4 (A) MALDI mass spectrum of a PEG 600 sample. (B) Ball and stick representation of the lowest energy structure for PEG_9Na^+. The O atoms are shown as the red circles and the C atoms as darker circles. H atoms are not shown and the Na^+ is represented in green. (C) Evolution of K_0^{-1} ($\propto$ CCS) as a function of the number of monomer units for a Na^+ cationized PEG chain. Open squares are experimental data while black circles are theoretical CCS computed from the MD-generated species. Adapted from Reference (von Helden et al., 1995b). CCS, collision cross section; MALDI, matrix-assisted laser desorption/ionization [Color figure can be viewed at wileyonlinelibrary.com]

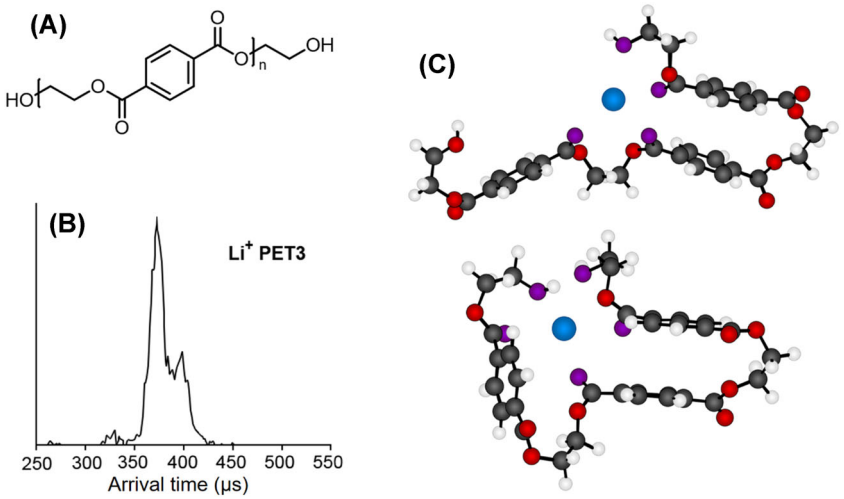

FIGURE 5 (A) Structure of PET. (B) ATD recorded for lithium adduct of PET_3 at room temperature. (C) Ball and stick representation of the opened and closed structures for $PET_nK^+$with $n = 3$. C atoms are shown in grey, O atoms in red and the K^+ ion in blue. O atoms coordinating the charge are shown in purple. Adapted from Reference (Gidden, Wyttenbach, et al., 1999). PET, poly(ethylene terephthalate) [Color figure can be viewed at wileyonlinelibrary.com]

structures, it appears that the interaction with Na^+ is different for the three polymers. In the case of 5-mers, six oxygen atoms are found to complex the charge irrespective of the nature of the backbone. For longer chains, the number of oxygen atoms complexing a Na^+ decreases from PEG to PTMEG (PEG > PPG > PTMEG) (Gidden et al., 2000). Indeed, the folding of PPG and PTMEG is hampered because of the longer distance between successive oxygen atoms. The nature and flexibility of the chain affect thus greatly the interaction between the polymer backbone and a charge, but always lead to a globular shape for larger chains.

The group of Bowers then went a step further by studying the conformation of poly(ethylene terephthalate)

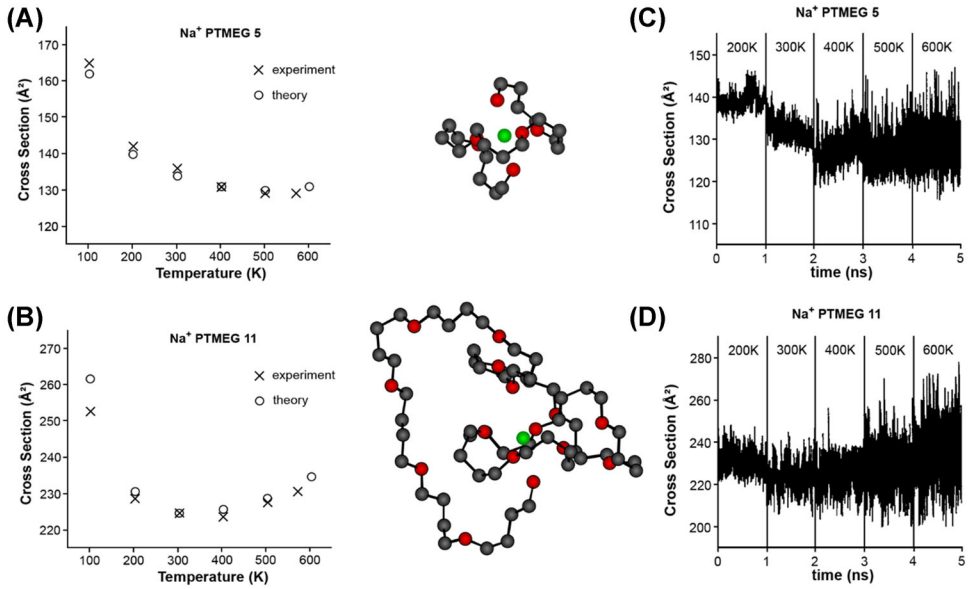

FIGURE 6 Left. Experimental CCS evolution of sodiated (A) PTMEG 5 and (B) PTMEG 11 as a function of temperature. Right. Time evolution of theoretical collision cross sections of sodiated PTMEG (5- and 11-mer) in a temperature variable molecular dynamics simulation. Representative structures of sodiated PTMEG 5- and 14-mer are also shown. Structural layout follows Figure 5. Adapted with permission from reference (Gidden et al., 2000). Copyright 2000 American Chemical Society [Color figure can be viewed at wileyonlinelibrary.com]

(PET) oligomers, thereby probing the conformation of singly charged oligomers with both floppy (ethylene) and rigid (phthalate) segments (Gidden, Jackson, et al., 1999; Gidden, Wyttenbach, et al., 1999). IMS-MS experiments were performed for oligomers PET_nM^+ with $n = 2$, 3, 4 and $M = Li^+$, Na^+ and K^+ (Figure 5A).

ATDs recorded for sodium and potassium adducts were unimodal and symmetric at room temperature, indicating either single conformers or fastly interconverting isomers. In contrast, ATDs recorded for PET_3Li^+ were found to be bimodal (Figure 5B) (Gidden, Jackson, et al., 1999; Gidden, Wyttenbach, et al., 1999). To interpret this result, MD simulations were conducted. MD-generated structures showed that π-stacking between adjacent aromatic rings constrains the structures of PET_2M^+ and PET_4M^+ while carbonyl oxygen atoms and terminal hydroxyl groups complex the charge. The 2- and 4-mers thus fold favorably around the charge so that two pairs of aromatic rings interact by π-stacking. However, only one pair of benzene rings can take part in π interactions in the 3-mer, leaving the third ring alone. The chain can therefore either remain extended or can fold completely around the charge with a terminal hydroxyl group playing a role in the complexation of the cation (Figure 5C). Interestingly, by lowering the temperature of the drift tube, a bimodal ATD also appeared for PET_3Na^+ at 80 K. At room temperature, the open and compact shapes thus probably coexist in the gas phase and are rapidly interconverting, resulting in a unimodal symmetric ATD. Using kinetic laws, the isomerization energy barrier was approached. In such a case, IMS-MS thus allowed to probe the interconversion dynamics between open and compact PET structures. It is also noteworthy that changing the power of the MALDI laser pulse modulates the shape of the ATDs, indicating that ion formation processes are susceptible to affect the ion shapes (Gidden, Wyttenbach, et al., 1999).

Finally, the flexible nature of the backbone of singly charged oligomers was further highlighted in temperature-dependent experiments. Indeed, compared to rigid compounds whose CCS decrease as the temperature increases due to weaker interactions between the ion and the buffer gas (Bleiholder et al., 2015), the CCS of polymer ions first decrease for similar reasons but then increase again (Gidden et al., 2000, 2001). To decipher this result, MD simulations were conducted at different temperatures. One of the advantages of MD simulations is the ability to provide kinetic energy to the system through a thermostat and thus to study the evolution of a system at different temperatures. The simulations conducted in the same range of temperatures (100–600 K) as the experiments showed that heating induces a high structural disorder and thus gives rise to a broader range of conformations including more extended conformations whose CCS are consequently larger (Figure 6) (Gidden et al., 2000; von Helden et al., 1995b).

As a summary, singly charged polymers adopt single loop or globular conformations as they fold around the cation by charge-dipole interactions. The resulting structures will heavily rely on the nature, flexibility and potential secondary noncovalent interactions.

3.3.2 | Multiply charged polymers

When additional cations are complexed to the polymer backbone, a completely different story ensues. Before diving into the MD simulations results of multiply charged polymers, we will shed light on the experimental evidence that motivated the support of MD simulations. In 2004, Ude et al. (2004) published the first IMS-MS analysis of multiply charged PEG ions using an ESI instrument. They analyzed various samples with M_n spanning from 200 to 50,000 Da to obtain a large range of PEG macroions with several charge states. IMS data recorded for ions with $1 < z < 12$ are summarized in Figure 7.

According to the Mason-Schamp equation (Equation 1), the z/K parameter (y axis in Figure 7) is directly proportional to the CCS. In addition, since the CCS of spherical objects evolves as a function of mass$^{2/3}$ (see Section 2) (Ruotolo et al., 2008), they fall on a straight line in this graph. Interestingly, irrespective of their charge state, the CCS of all PEG ions eventually fall on the same spherical evolution at larger masses. This indicates that, regardless of their charge state, multiply charged PEG ions can adopt a spherical shape provided that their mass is high enough (Ude et al., 2004).

Starting from a spherical structure at high mass with a given charge z, the CCS drastically increases if the mass decreases below a critical mass $m^*(z)$. This indicates that gaseous ions adopt a more extended conformation. Based on their PEG data, the authors measured the critical mass $m^*(z)$ for $z = 2, 3, 4, 5$ (Table 1).

Interestingly, while m^* increases with z, m^*/z^2 remains roughly constant. This is in full consistency with the Rayleigh limit, that corresponds to the balance between electrostatic repulsion and surface tension in a charged droplet (Rayleigh, 1882). As the Coulombic repulsion overcomes the surface tension, the droplet becomes unstable and ejects a charge. The Rayleigh limit is the maximum number of charges z_R a liquid droplet can contain before electrostatic instability and is described by Equation (8) in which e is the elementary charge, ε_0 the vacuum permittivity, γ the droplet surface tension and R the droplet radius (Konermann et al., 2013).

$$z_R = \frac{8\pi}{e}\sqrt{\varepsilon_0 \gamma R^3}. \tag{8}$$

By substituting $\sqrt{R^3}$ by the density $= \frac{m}{V} = \frac{3m}{4\pi R^3}$, the following equation can be obtained:

TABLE 1 Critical masses m^* and m^*/z^2 for PEG ions with different charge states (Ude et al., 2004)

z	2	3	4	5
m^* (amu)	1991	4435	8024	12,666
m^*/z^2	497.7	492.8	501.5	506.6

Note: Reprinted with permission from reference (Ude et al., 2004). Copyright 2004 American Chemical Society.

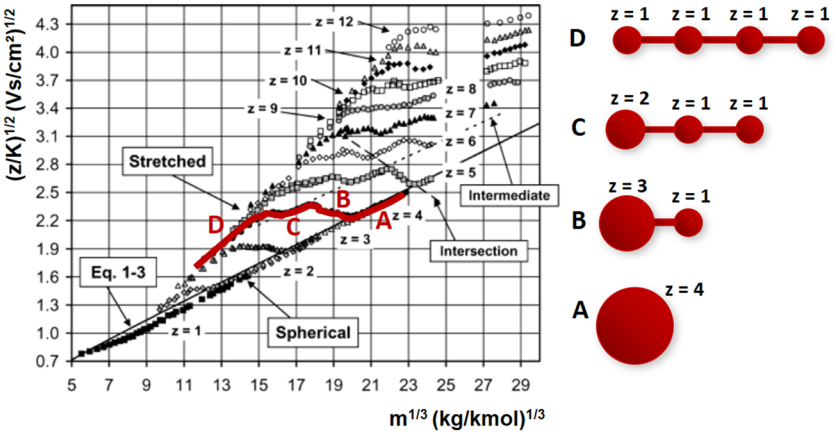

FIGURE 7 Mobility data recorded for PEG macroions complexed with 1–12 ammonium ions. The evolution of the mobility data for quadruply charged ions are highlighted in red along with sketches representing candidate structures derived from MD simulations. Adapted with permission from references (Larriba & Fernandez De La Mora, 2012; Ude et al., 2004). Copyright 2004, 2012 American Chemical Society (Larriba & Fernandez De La Mora, 2012; Ude et al., 2004). MD, molecular dynamics; PEG, poly(ethylene glycol) [Color figure can be viewed at wileyonlinelibrary.com]

$$\frac{m}{z_R^2} = \frac{1}{48\pi}\frac{e^2\rho}{\gamma\varepsilon_0}. \quad (9)$$

By considering spherical PEG ions as charged droplets with a density ρ, a coulombic instability should appear below a given m/z^2 ratio, consistent with the data in Table 1. The CCS increase observed in Figure 7 for ions with $m(z) < m^*(z)$ thus points to a charge-induced instability resulting in the modification of the ion shape. This "unfolding" can be compared to a charge ejection from a coulombically unstable droplet (Larriba & Fernandez De La Mora, 2012; Ude et al., 2004). For ions with $z > 2$, further instabilities are expected for critical masses lower than $m^*(z)$. Based on this interpretation, it was proposed that each inflection point in the CCS evolution of an ion with a given charge z can be associated to charge-induced instabilities. The monotonic evolutions at low masses are associated to completely stretched conformations (also called "beads-on-a-string") and the monotonic evolution at high masses correspond to globular species, while the in-between conformations remain to be identified.

As an example, the CCS evolution of quadruply charged PEG ions are highlighted in Figure 7. In this figure, (A) was proposed to correspond to a spherical structure while (D) is associated to a "beads-on-a-string" conformation. Other intermediate conformers were pointed out but not yet formally identified. To provide a complete picture, Trimpin and Clemmer led a joint IMS/MD work in 2007 on Cs^+-coordinated PEGs (Trimpin et al., 2007). Their MD results were coherent with the speculations made on the experimental data, that is, large PEG chains adopt compact structures (A) while smaller highly charged oligomers adopt extended structures (D). In 2011, our group reported a joint IMS/MD investigation of the gas-phase behavior of sodiated polylactide (PLA) ions with $z = 2$ and 3 (De Winter et al., 2011). All detected PLA ions followed the trend established by Ude et al. (2004) Indeed, 2+ PLA ions were found to adopt globular structures for larger masses ($m > m^*(z)$) while smaller chains adopted stretched conformations because of a charge-induced instability. Interestingly, MD simulations allowed to identify the intermediate structures ($m^{**}(z) < m < m^*(z)$) of 3+ PLA ions. These intermediate shapes are constituted of a doubly charged globule bearing a singly charged appendix (De Winter et al., 2011). In 2012, Larriba and De La Mora also performed MD simulations to identify the intermediate PEG structures (B and C) pictured in Figure 7 (Larriba & Fernandez De La Mora, 2012). Consistent with PLA data, they obtained structures by a multiply charged globule bearing a singly or multiply charge appendix. While globules bearing a single appendix are pictured in Figure 7, the postulate of other intermediate structures like (C) but composed of a multiply charged globule bearing several singly charged appendices pointing in different directions could not be ruled out (Larriba & Fernandez De La Mora, 2012). Similar intermediate structures were also obtained through MD simulations by Morsa et al. and Haler et al. on multiply charged poly (ε-caprolactone), and poly(ethoxy phosphate) chains (Haler et al., 2020; Morsa et al., 2014).

To summarize, depending on their charge z and length L (or mass m), polymer ions can adopt single or multiple conformations in the gas phase, with the maximum number of conformational families generally equal to z. The gas-phase structure of multiply charged polymer ions is governed by the ratio between their charge state and chain length z/L. For very high z/L, polymer ions will adopt a "beads-on-a-string" structure. For longer chains, intermediate structures characterized by inflection points in CCS/mass or CCS/DP evolutions are detected. Finally, for sufficiently low z/L, all polymer ions adopt a globular conformation, regardless of their charge.

The peculiar gas-phase behavior of multiply charged polymer ions is generally at the origin of the IMS separation of isomeric polymers. Indeed, singly charged polymer ions adopt globular conformations, making troublesome the distinction between architecturally different polymers by IMS-MS (Baker et al., 2004). As a result, the IMS-MS separation of linear/cyclic isomers (Hoskins et al., 2011; Liénard et al., 2020), of star-shaped topologies (Austin et al., 2021; Foley et al., 2015; Morsa et al., 2011) and of copolymers with different sequences (Duez, Moins, et al., 2020; Ito et al., 2019) was only reported for multiply charged ions.

3.4 | Explicit simulation of ion mobility

The modeling approaches detailed in the paragraphs (*a*) and (*b*) are carried out on conformations sampled either by quantum or classical methods. Another method developed by Lai et al. (2018) consists in simulating the behavior of an ion in a drift tube mobility cell by considering the gas explicitly and applying an electric field onto the system. This new type of simulation has the asset to directly sample conformations while performing "on-the-fly" the ion mobility analysis, thereby providing a more realistic description. With this method, the conformational and temperature effects are explicitly considered. In practice, the trajectory of an ion is simulated in Periodic Boundary Conditions inside a box filled with several hundreds of gas molecules. To simulate the motion of an ion for a shorter time than an IMS experiment

(~10 ms), the simulation is performed with a higher pressure and electric field than experimentally, while keeping an *E/N* ratio reasonably low. This allows to shorten the simulation down to reasonable computation times. This method has proven very efficient for relatively small ions (<100 atoms), and provides close results compared to the gold standard "Trajectory Method" (Lai et al., 2018).

However, this appealing method was reported very recently and only used in two reports (Gelb et al., 2019; Lai et al., 2018). Its applicability to a larger range of compounds, including synthetic polymers, still needs to be demonstrated.

3.5 | Influence of ion production: Electrospray droplet simulations

While MD simulations in vacuum generally provide a very nice agreement with experimental data from polymer ions, the interpretation of experimental evidence linked to dynamic events in gas phase can reveal tricky. Indeed, the observation of unimodal ATDs can be attributed to both the coexistence of ions having a single family of conformations in gas phase, or to rapidly interconverting conformers (Poyer et al., 2017). In the field of polymers, the hypothesis of rapidly interconverting conformers has been proposed for doubly charged poly (ethoxy phosphate) and poly(propiolactone) ions based on MD simulations (Duez, Moins, et al., 2020; Haler et al., 2020). Indeed, at the time scale of the MD simulation (~ns), interconverting conformers can be generated and lead to bimodal CCS_{th} distributions whose center coincide with experimental values. On the other hand, when bimodal ATDs are recorded, they are generally attributed to noninterconverting conformers.

Our group recently reported that multiply charged PLA ions involved in structural transitions can be detected with multimodal ATDs, hinting the coexistence of multiple coexisting conformations in gas phase (Duez, Josse, et al., 2017). Tandem IMS experiments involving collisional activation revealed the remarkable kinetic stability of these conformers. Indeed, by selecting ion conformations after a first stage of IMS separation and submitting them to collisional activation, no structural change was observed. Other studies on poly(ethoxy phosphate) ions also revealed that these polymers are not prone to CIU (Haler et al., 2018). It was thus proposed that our PLA ions are produced with a given conformation in the ESI ion source and retain their structure throughout the entire instrument. In addition, ion production conditions in the ESI source were found to impact the relative proportions of these conformations (Duez, Josse, et al., 2017). A similar effect was observed by Gidden, Wyttenbach, et al. (1999) when changing the laser pulse of their MALDI-IMS instrument. In this case, "simple" gas-phase sampling by MD simulations will not be suitable to decipher the structure of these coexisting conformers. Indeed, the simulation of two non-interconverting structures would require running many simulations from different starting points.

A similar problem was encountered by Porrini et al. (2017) who studied the compaction of DNA duplexes by IMS-MS and MD simulations. Unbiased gas-phase MD simulations and Replica Exchange MD (REMD) simulations were performed on solvent-stripped DNA-duplexes, and both failed to converge to the experimentally sampled structure. Indeed, a phosphate-phosphate hydrogen bond network rearranges during the transfer from solution to gas phase and cannot be accurately sampled by vacuum MD simulations nor REMD. To cope with this issue, Porrini et al. (2017) modelled the progressive evaporation of ESI droplets by MD, which lead to more realistic structures. Later, Khristenko et al. (2019) proposed that ESI ion production mechanisms may impact a balance between extended versus compact structures for nucleic acids. It thus appears that ion production mechanisms may not always be ignored to break down the conformation of gaseous ions.

The MD simulation of polymer-containing ESI droplets was pioneered by Consta and coworkers (Chung & Consta, 2012; Consta & Chung, 2011; Soltani et al., 2015). Their work, focused on the release of PEG ions, showed the progressive migration of the polymer chain to the surface of droplet followed by a progressive extrusion of the chain after complexation with cations. At this point, the chain either remains on the surface of the droplet until evaporation to dryness or is expelled in the gas phase, in agreement with the Chain Ejection Model (CEM) and Charge Residue Model (CRM) (Ahadi & Konermann, 2012; McAllister et al., 2015). The first joint IMS/MD investigation of the ESI release of polymer ions was carried out for PPG and reported similar results, with an excellent agreement between experimental and MD-produced charge states and CCS (Duez et al., 2018). Following procedures established in the laboratory of Lars Konermann, our group investigated the release of PLA ions by MD simulations of evaporating ESI droplets. For a subset of ions that are detected with bimodal ATDs, associated with kinetically stable conformers (Duez, Josse, et al., 2017), the simulation of evaporating PLA-containing ESI droplets generated two ion structures that matched experimentally sampled structures (Duez, Metwally, et al., 2020). These two nascent ions, that is, directly after release from droplets, did not show any interconversion in subsequent gas-phase simulations. Interestingly, a correlation could be observed between ESI

release mechanisms and gas-phase conformations. The compact ion shapes appeared to arise from the CRM while extended conformations were obtained from the CEM. For this subset of ions, ionization processes result in specific structural features.

Altogether, while unbiased vacuum MD is suitable to describe most systems, the impact of ionization and transfer to gas-phase may not always be ignored to fully interpret experimental results. With continuous improvement in computer hardware and MD software, it is hoped that new simulation strategies embedding both ionization and gas-phase relaxation will be developed in the future to better interpret IMS-MS results.

4 | CONCLUSIONS

The development of soft ionization sources during the 80's paved the way for the investigation of macromolecules by MS. It then became possible to characterize the structure and mass parameters of intact polymers with various topologies. Along with multistage MS, IMS is increasingly used for the structural characterization of gaseous polymer ions. Given their intrinsic dispersity ($Đ_M > 1.00$), most IMS-MS investigations of polymers focus on the evolution of IMS signals throughout the chain distribution. To rationalize the recorded data, many ways have been proposed. This review reports about two of them, namely IMS data fittings and atomistic simulations.

First, we reviewed procedures to fit IMS datasets. These approaches have been employed to determine physicochemical parameters of polymer ions, such as the characteristic ratio or relative dielectric constant, and to approach their gas-phase structure. However, IMS data set fitting can cause to misleading interpretations, especially for the fitting of data belonging to non-globular ions.

Atomistic simulations were then described to interpret the gas-phase structure polymer ions. A general workflow, including generation of candidate structures and CCS simulation, was described. QM methods, including DFT, were reported for the description of the structure of small singly-cationized oligomers. Due to the high computational cost of QM approaches, MD simulations were rather employed for multiply charged polymers. Many examples of joint IMS/MD approaches have been reported, yet vacuum simulations do not account for effects of ion production mechanisms. In this case, strategies to model ESI processes, including droplet evaporation and ionization mechanisms, were reported with excellent agreement between MD-generated conformations and IMS-MS experiments.

Overall, atomistic simulations appear as the ideal companion for the interpretation of IMS-MS data. Most of the data discussed in the present review relate to synthetic polymers whose solution structure does not follow any specific organization, due to their intrinsic flexibility. One of the next challenges in the field will probably be the analysis of polymers whose secondary structure directly relates to their sequence and composition. Provided that these secondary structures are conserved during ionization and desolvation processes, the primary structure of polymers would be directly deduced from the analysis of their conformation in gas-phase, making IMS-MS the ideal technique for polymer characterization and identification.

ACKNOWLEDGMENTS

Quentin Duez thanks the FNRS for his PhD grant. Sébastien Hoyas thanks the "Fonds pour la Recherche Industrielle et Agricole" for his PhD grant. Jérôme Cornil is a FNRS research fellow.

REFERENCES

Ahadi, E, & Konermann, L. Modeling the behavior of coarse-grained polymer chains in charged water droplets: Implications for the mechanism of electrospray ionization. *J. Phys. Chem. B* 2012;*116*(1):104–112.

Alessi, ML, Norman, AI, Knowlton, SE, Ho, DL, & Greer, SC. Helical and coil conformations of poly(ethylene glycol) in isobutyric acid and water. *Macromolecules* 2005;*38*(22): 9333–9340.

Alexander, NE, Swanson, JP, Joy, A, & Wesdemiotis, C. Sequence analysis of cyclic polyester copolymers using ion mobility tandem mass spectrometry. *Int. J. Mass Spectrom*. 2018;*429*: 151–157.

Allen, G, Booth, C, Hurst, SJ, Jones, MN, & Price, C. Intrinsic viscosity and light scattering measurements on poly(ethylene oxide), poly(styrene oxide) and poly(t-butyl ethylene oxide). *Polymer*. 1967;*8*:391–397.

Amalian, J-A, Cavallo, G, Al Ouahabi, A, Lutz, J-F, & Charles, L. Revealing data encrypted in sequence-controlled poly(alkoxyamine phosphodiester)s by combining ion mobility with tandem mass spectrometry. *Anal. Chem*. 2019;*91*(11): 7266–7272.

Anderson, SE, Baker, ES, Mitchell, C, Haddad, TS, & Bowers, MT. Structure of hybrid polyhedral oligomeric silsesquioxane propyl methacrylate oligomers using ion mobility mass spectrometry and molecular mechanics. *Chem. Mater*. 2005;*17*(10): 2537–2545.

Anderson, SE, Bleiholder, C, Brocker, ER, Stang, PJ, & Bowers, MT. A novel projection approximation algorithm for the fast and accurate computation of molecular collision cross sections (III): Application to supramolecular coordination-driven assemblies with complex shapes. *Int. J. Mass Spectrom*. 2012;*332*:78–84.

Atkins, P, & Friedman, R. Molecular quantum mechanics (5th ed.). Oxford University Press. 2011.

Austin, CA, Inutan, ED, Bohrer, BC, Li, J, Fischer, JL, Wijerathne, K, Foley, CD, Lietz, CB, Woodall, DW, Imperial, LF, Clemmer, DE, Trimpin, S, & Larsen, BS. Resolving isomers of star-branched poly(ethylene glycols) by IMS-MS using multiply charged ions. *J. Am. Soc. Mass Spectrom*. 2021;*32*(1):21–32.

Baker, ES, Gidden, J, Simonsick, WJ, Grady, MC, & Bowers, MT. Sequence dependent conformations of glycidyl methacrylate/butyl methacrylate copolymers in the gas phase. *Int. J. Mass Spectrom*. 2004;*238*(3):279–286.

Bannwarth, C, Caldeweyher, E, Ehlert, S, Hansen, A, Pracht, P, Seibert, J, Spicher, S, & Grimme, S. Extended tight-binding quantum chemistry methods. *WIREs Comput. Mol. Sci*. 2021;*11*(2):1–49.

Barner-Kowollik, C, Gruendling, T, Falkenhagen, J, Robert, T, & Michael, AR. Mass spectrometry in polymer chemistry. Wiley-VCH. 2012.

Barrère, C, Selmi, W, Hubert-Roux, M, Coupin, T, Assumani, B, Afonso, C, & Giusti, P. Rapid analysis of polyester and polyethylene blends by ion mobility-mass spectrometry. *Polym. Chem*. 2014;*5*(11):3576–3582.

Beech, DR, & Booth, C. Unperturbed dimensions of poly(ethylene oxide). *J. Polym. Sci. Part A-2 Polym. Phys*. 1969;*7*(3):575–586.

Bleiholder, C. A local collision probability approximation for predicting momentum transfer cross sections. *Analyst* 2015;*140*(20):6804–6813.

Bleiholder, C, Contreras, S, & Bowers, MT. A novel projection approximation algorithm for the fast and accurate computation of molecular collision cross sections (IV). Application to polypeptides. *Int. J. Mass Spectrom*. 2013;*354-355*:275–280.

Bleiholder, C, Contreras, S, Do, TD, & Bowers, MT. A novel projection approximation algorithm for the fast and accurate computation of molecular collision cross sections (II). Model parameterization and definition of empirical shape factors for proteins. *Int. J. Mass Spectrom*. 2013;*345-347*:89–96.

Bleiholder, C, Johnson, NR, Contreras, S, Wyttenbach, T, & Bowers, MT. Molecular structures and ion mobility cross sections: Analysis of the effects of He and N2 buffer gas. *Anal. Chem*. 2015;*87*(14):7196–7203.

Bleiholder, C, Wyttenbach, T, & Bowers, MT. A novel projection approximation algorithm for the fast and accurate computation of molecular collision cross sections (I). Method. *Int. J. Mass Spectrom*. 2011;*308*(1):1–10.

Bornschein, RE, Hyung, SJ, & Ruotolo, BT. Ion mobility-mass spectrometry reveals conformational changes in charge reduced multiprotein complexes. *J. Am. Soc. Mass Spectrom*. 2011;*22*(10):1690–1698.

Borysik, AJH, Radford, SE, & Ashcroft, AE. Co-populated conformational ensembles of β2microglobulin uncovered quantitatively by electrospray ionization mass spectrometry. *J. Biol. Chem*. 2004;*279*(26):27069–27077.

Bradt, P, Dibeler, VH, & Mohler, FL. A new technique for the mass spectrometric study of the pyrolysis products of polystyrene. *J. Res. Natl. Bur. Stand*. 1953;*50*(4):201.

Broch, K, Venkateshvaran, D, Lemaur, V, Olivier, Y, Beljonne, D, Zelazny, M, Nasrallah, I, Harkin, DJ, Statz, M, Pietro, R Di, Kronemeijer, AJ, & Sirringhaus, H. Measurements of ambipolar seebeck coefficients in high-mobility diketopyrrolopyrrole donor-acceptor copolymers. *Adv. Electron. Mater*. 2017;*3*(11):1700225.

Campuzano, I, Bush, MF, Robinson, C V, Beaumont, C, Richardson, K, Kim, H, & Kim, HI. Structural characterization of drug-like compounds by ion mobility mass spectrometry: Comparison of theoretical and experimentally derived nitrogen collision cross sections. *Anal. Chem*. 2012;*84*(2):1026–1033.

Charles, L, Chendo, C, & Poyer, S. Ion mobility spectrometry–Mass spectrometry coupling for synthetic polymers. *Rapid Commun. Mass Spectrom*. 2020;*34*(S2):1–23.

Chen, Z, Glover, MS, & Li, L. Recent advances in ion mobility–mass spectrometry for improved structural characterization of glycans and glycoconjugates. *Curr. Opin. Chem. Biol*. 2018;*42*:1–8.

Chung, JK, & Consta, S. Release mechanisms of poly(ethylene glycol) macroions from aqueous charged nanodroplets. *J. Phys. Chem. B* 2012;*116*(19):5777–5785.

Consta, S, & Chung, JK. Charge-induced conformational changes of PEG-(Na+)n in a vacuum and aqueous nanodroplets. *J. Phys. Chem. B* 2011;*115*:10447–10455.

Craig, B, Skylaris, CK, Schoetz, T, & de León, CP. A computational chemistry approach to modelling conducting polymers in ionic liquids for next generation batteries. *Energy Reports* 2020;*6*:198–208.

Crescentini, TM, May, JC, McLean, JA, & Hercules, DM. Alkali metal cation adduct effect on polybutylene adipate oligomers: Ion mobility-mass spectrometry. *Polymer*. 2019;*173*:58–65.

Crotty, S, Gerislioglu, S, Endres, KJ, Wesdemiotis, C, & Schubert, U. Polymer architectures via mass spectrometry and hyphenated techniques: A review. *Anal. Chim. Acta* 2016;*932*:1–21.

Daly, S, Rosu, F, & Gabelica, V. Mass-resolved electronic circular dichroism ion spectroscopy. *Science*. 2020;*368*(6498):1465–1468.

Davison, WHTS, Slaney, S, & Wragg, AL. A novel method of identification of polymers. *Chem. Ind*. 1954;1356.

de Hoffmann, E, & Stroobant, V. Mass spectrometry: Principles and applications (3rd ed.) Wiley. 2007.

Dixit, SM, Polasky, DA, & Ruotolo, BT. Collision induced unfolding of isolated proteins in the gas phase: Past, present, and future. *Curr. Opin. Chem. Biol*. 2018;*42*:93–100.

Dubois, P, Coulembier, O, & Raquez, J. Handbook of ring-opening polymerization (P. Dubois, O. Coulembier, & J. Raquez (Eds.)). Wiley. 2009.

Duez, Q, Chirot, F, Liénard, R, Josse, T, Choi, C, Coulembier, O, Dugourd, P, Cornil, J, Gerbaux, P, & De Winter, J. Polymers for traveling wave ion mobility spectrometry calibration. *J. Am. Soc. Mass Spectrom*. 2017;*28*(11):2483–2491.

Duez, Q, van Huizen, NA, Lemaur, V, De Winter, J, Cornil, J, Burgers, PC, & Gerbaux, P. Silver ion induced folding of alkylamines observed by ion mobility experiments. *Int. J. Mass Spectrom*. 2019;*435*:34–41.

Duez, Q, Josse, T, Lemaur, V, Chirot, F, Choi, CM, Dubois, P, Dugourd, P, Cornil, J, Gerbaux, P, & De Winter, J. Correlation between the shape of the ion mobility signals and the stepwise folding process of polylactide ions. *J. Mass Spectrom*. 2017;*52*(3):133–138.

Duez, Q, Liénard, R, Moins, S, Lemaur, V, Coulembier, O, Cornil, J, Gerbaux, P, & De Winter, J. One step further in the

characterization of synthetic polymers by ion mobility mass spectrometry: Evaluating the contribution of end-groups. *Polymers*. 2019;*11*(4):688.

Duez, Q, Metwally, H, Hoyas, S, Lemaur, V, Cornil, J, De Winter, J, Konermann, L, & Gerbaux, P. Effects of electrospray mechanisms and structural relaxation on polylactide ion conformations in the gas phase: Insights from ion mobility spectrometry and molecular dynamics simulations. *Phys. Chem. Chem. Phys*. 2020;*22*(7):4193–4204.

Duez, Q, Metwally, H, & Konermann, L. Electrospray ionization of polypropylene glycol: Rayleigh-charged droplets, competing pathways, and charge state-dependent conformations. *Anal. Chem*. 2018;*90*(16):9912–9920.

Duez, Q, Moins, S, Coulembier, O, De Winter, J, Cornil, J, & Gerbaux, P. Assessing the structural heterogeneity of isomeric homo and copolymers: An approach combining ion mobility mass spectrometry and molecular dynamics simulations. *J. Am. Soc. Mass Spectrom*. 2020;*31*(11):2379–2388.

Ewing, MA, Glover, MS, & Clemmer, DE. Hybrid ion mobility and mass spectrometry as a separation tool. *J. Chromatogr. A*. 2016;*1439*:3–25.

Ewing, SA, Donor, MT, Wilson, JW, & Prell, JS. Collidoscope: An improved tool for computing collisional cross-sections with the trajectory method. *J. Am. Soc. Mass Spectrom*. 2017;*28*(4): 587–596.

Foley, CD, Zhang, B, Alb, AM, Trimpin, S, & Grayson, SM. Use of ion mobility spectrometry-mass spectrometry to elucidate architectural dispersity within star polymers. *ACS Macro Lett*. 2015;*4*(7):778–782.

Frerichs, N, Joswig, M, Fischer, TL, Oevermann, YS, & Vana, P. Elucidating the topology and physical properties of triblock copolymers using ion mobility mass spectrometry. *Macromol. Chem. Phys*. 2021;*222*(1):2000317.

Gabelica, V, & Marklund, E. Fundamentals of ion mobility spectrometry. *Curr. Opin. Chem. Biol*. 2018;*42*(2):51–59.

Gabelica, V, Shvartsburg, AA, Afonso, C, Barran, PE, Benesch, JLP, Bleiholder, C, Bowers, MT, Bilbao, A, Bush, MF, Campbell, JL, Campuzano, IDG, Causon, T, Clowers, BH, Creaser, CS, De Pauw, E, Far, J, Fernandez-Lima, F, Fjeldsted, JC, Giles, K, Groessl, M, Hogan, CJ, Hann, S, Kim, HI, Kurulugama, RT, May, JC, McLean, JA, Pagel, K, Richardson, K, Ridgeway, ME, Rosu, F, Sobott, F, Thalassinos, K, Valentine, SJ, & Wyttenbach, T. Recommendations for reporting ion mobility mass spectrometry measurements. *Mass Spectrom. Rev*. 2019; *38*(3):291–320.

Gaborieau, M, & Castignolles, P. Size-exclusion chromatography (SEC) of branched polymers and polysaccharides. *Anal. Bioanal. Chem*. 2011;*399*(4):1413–1423.

Gelb, AS, Lai, R, Li, H, & Dodds, ED. Composition and charge state influence on the ion-neutral collision cross sections of protonated N-linked glycopeptides: An experimental and theoretical deconstruction of coulombic repulsion vs. charge solvation effects. *Analyst* 2019;*144*(19):5738–5747.

Gidden, J, Bowers, MT, Jackson, AT, & Scrivens, JH. Gas-phase conformations of cationized poly(styrene) oligomers. *J. Am. Soc. Mass Spectrom*. 2002;*13*(5):499–505.

Gidden, J, Bushnell, JE, & Bowers, MT. Gas-phase conformations and folding energetics of oligonucleotides: dTG - and dGT -. *J. Am. Chem. Soc*. 2001;*123*(23):5610–5611.

Gidden, J, Jackson, AT, Scrivens, JH, & Bowers, MT. Gas phase conformations of synthetic polymers: Poly (methyl methacrylate) oligomers cationized by sodium ions. *Int. J. Mass Spectrom*. 1999;*188*:121–130.

Gidden, J, Wyttenbach, T, Batka, JJ, Weis, P, Bowers, MT, Jackson, AT, & Scrivens, JH. Poly (ethylene terephthalate) oligomers cationized by alkali ions: Structures, energetics, and their effect on mass spectra and the matrix-assisted laser desorption/ionization process. *J. Am. Soc. Mass Spectrom*. 1999;*10*(9):883–895.

Gidden, J, Wyttenbach, T, Jackson, AT, Scrivens, JH, & Bowers, MT. Gas-phase conformations of synthetic polymers: Poly(ethylene glycol), poly(propylene glycol), and poly(tetramethylene glycol). *J. Am. Chem. Soc*. 2000;*122*(19):4692–4699.

Haler, JRN, Far, J, De La Rosa, VR, Kune, C, Hoogenboom, R, & De Pauw, E. Using ion mobility-mass spectrometry to extract physicochemical enthalpic and entropic contributions from synthetic polymers. *J. Am. Soc. Mass Spectrom*. 2021;*32*(1): 330–339.

Haler, JRN, Lemaur, V, Far, J, Kune, C, Gerbaux, P, Cornil, J, & De Pauw, E. Sodium coordination and protonation of poly (ethoxy phosphate) chains in the gas phase probed by ion mobility-mass spectrometry. *J. Am. Soc. Mass Spectrom*. 2020; *31*(3):633–641.

Haler, JRN, Massonnet, P, Chirot, F, Kune, C, Comby-Zerbino, C, Jordens, J, Honing, M, Mengerink, Y, Far, J, Dugourd, P, & De Pauw, E. Comparison of different ion mobility setups using poly (ethylene oxide) PEO polymers: Drift tube, TIMS, and T-wave. *J. Am. Soc. Mass Spectrom*. 2017;*29*:114–120.

Haler, JRN, Massonnet, P, Far, J, de la Rosa, VR, Lecomte, P, Hoogenboom, R, Jérôme, C, & De Pauw, E. Gas-phase dynamics of collision induced unfolding, collision induced dissociation, and electron transfer dissociation-activated polymer ions. *J. Am. Soc. Mass Spectrom*. 2018; *30*(4):563–572.

Haler, JRN, Massonnet, P, Far, J, Upert, G, Gilles, N, Mourier, G, Quinton, L, & De Pauw, E. Can IM-MS collision cross sections of biomolecules be rationalized using collision cross-section trends of polydisperse synthetic homopolymers? *J. Am. Soc. Mass Spectrom*. 2020;*31*(4):990–995.

Haler, JRN, Morsa, D, Lecomte, P, Jérôme, C, Far, J, & De Pauw, E. Predicting Ion Mobility-Mass Spectrometry trends of polymers using the concept of apparent densities. *Methods* 2018;*144*: 125–133.

Hanton, SD. Mass spectrometry of polymers and polymer surfaces. *Chem. Rev*. 2001;*101*(2):527–569.

von Helden, G, Hsu, MT, Gotts, N, & Bowers, MT. Carbon cluster cations with up to 84 atoms: Structures, formation mechanism, and reactivity. *J. Phys. Chem*. 1993;*97*(31):8182–8192.

von Helden, G, Wyttenbach, T, & Bowers, MT. Conformation of macromolecules in the gas phase: Use of matrix-assisted laser desorption methods in ion chromatography. *Science*. 1995a; *267*(5203):1483–1485.

von Helden, G, Wyttenbach, T, & Bowers, MT. Inclusion of a MALDI ion source in the ion chromatography technique: Conformational information on polymer and biomolecular ions. *Int. J. Mass Spectrom. Ion Process*. 1995b;*146-147*: 349–364.

Hopper, JTS, & Oldham, NJ. Collision induced unfolding of protein ions in the gas phase studied by ion mobility-mass

spectrometry: The effect of ligand binding on conformational stability. *J. Am. Soc. Mass Spectrom*. 2009;*20*(10):1851–1858.

Hoskins, JN, Trimpin, S, & Grayson, SM. Architectural differentiation of linear and cyclic polymeric isomers by ion mobility spectrometry-mass spectrometry. *Macromolecules* 2011; *44*(17):6915–6918.

Hoyas, S, Halin, E, Lemaur, V, De Winter, J, Gerbaux, P, & Cornil, J. Helicity of peptoid ions in the gas phase. *Biomacromolecules* 2020;*21*:903–909.

Hoyas, S, Lemaur, V, Duez, Q, Saintmont, F, Halin, E, De Winter, J, Gerbaux, P, & Cornil, J. PEPDROID: Development of a generic DREIDING-based force field for the assessment of peptoid secondary structures. *Adv. Theory Simulations* 2018;*1*(12): 1800089.

Hudgins, RR, & Jarrold, MF. Helix formation in unsolvated alanine-based peptides: Helical monomers and helical dimers. *J. Am. Chem. Soc*. 1999;*121*(14):3494–3501.

Hudgins, RR, Mao, Y, Ratner, MA, & Jarrold, MF. Conformations of Gly(n)H+and Ala(n)H+peptides in the gas phase. *Biophys. J*. 1999;*76*(3):1591–1597.

Huijser, S, Staal, BBP, Huang, J, Duchateau, R, & Koning, CE. Chemical composition and topology of poly(lactide-co-glycolide) revealed by pushing MALDI-TOF MS to its limit. *Angew. Chemie* 2006;*118*(25):4210–4214.

Ieritano, C, Crouse, J, Campbell, JL, & Hopkins, WS. A parallelized molecular collision cross section package with optimized accuracy and efficiency. *Analyst* 2019;*144*(5):1660–1670.

Ito, K, Kitagawa, S, & Ohtani, H. Analysis of multiply charged poly (ethylene oxide- co -propylene oxide) using electrospray ionization–ion mobility spectrometry–mass spectrometry. *Anal. Sci*. 2019;*35*:169–174.

Izunobi, JU, & Higginbotham, CL. Polymer molecular weight analysis by ^{1}H NMR spectroscopy. *J. Chem. Educ*. 2011:*88*(8): 1098–1104.

Jackson, AT, Scrivens, JH, Williams, JP, Baker, ES, Gidden, J, & Bowers, MT. Microstructural and conformational studies of polyether copolymers. *Int. J. Mass Spectrom*. 2004;*238*(3): 287–297.

Jas, GS, & Kuczera, K. Equilibrium structure and folding of a helix-forming peptide: Circular dichroism measurements and replica-exchange molecular dynamics simulations. *Biophys. J*. 2004;*87*(6):3786–3798.

Jašík, J, Žabka, J, Roithová, J, & Gerlich, D. Infrared spectroscopy of trapped molecular dications below 4K. *Int. J. Mass Spectrom*. 2013;*354-355*:204–210.

Johansson, MP, Kaila, VRI, & Sundholm, D. Ab initio, density functional theory, and semi-empirical calculations. Methods Mol. Biol. 2013;*924*:3-27.

Josse, T, De Winter, J, Dubois, P, Coulembier, O, Gerbaux, P, & Memboeuf, A. A tandem mass spectrometry-based method to assess the architectural purity of synthetic polymers: A case of a cyclic polylactide obtained by click chemistry. *Polym. Chem*. 2015;*6*(1):64–69.

Jurneczko, E, & Barran, PE. How useful is ion mobility mass spectrometry for structural biology? the relationship between protein crystal structures and their collision cross sections in the gas phase. *Analyst* 2011;*136*(1):20–28.

Karas, M, Bachmann, D, & Hillenkamp, F. Influence of the wavelength in high-irradiance ultraviolet laser desorption mass spectrometry of organic molecules. *Anal. Chem*. 1985;*57*(14): 2935–2939.

Karas, M, & Hillenkamp, F. Laser desorption ionization of proteins with molecular masses exceeding 10,000 daltons. *Anal. Chem*. 1988;*60*(20):2299–2301.

Karas, M, & Krüger, R. Ion formation in MALDI: The cluster ionization mechanism. *Chem. Rev*. 2003;*103*(2):427–440.

Khristenko, N, Amato, J, Livet, S, Pagano, B, Randazzo, A, & Gabelica, V. Native ion mobility mass spectrometry: When gas-phase ion structures depend on the electrospray charging process. *J. Am. Soc. Mass Spectrom*. 2019;*30*(6):1069–1081.

Kim, K, Lee, JW, Chang, T, & Kim, HI. Characterization of polylactides with different stereoregularity using electrospray ionization ion mobility mass spectrometry. *J. Am. Soc. Mass Spectrom*. 2014;*25*:1771–1779.

Kohtani, M, Jarrold, MF, Wee, S, & O'Hair, RAJ. Metal ion interactions with polyalanine peptides. *J. Phys. Chem. B* 2004; *108*(19):6093–6097.

Kokubo, S, & Vana, P. Easy access to the characteristic ratio of polymers using ion-mobility mass spectrometry. *Macromol. Chem. Phys*. 2016;*218*(1):1600373.

Kokubo, S, & Vana, P. Obtaining the dielectric constant of polymers from doubly charged species in ion-mobility mass spectrometry. *Macromol. Chem. Phys*. 2017;*218*(17):1700126.

Konermann, L, Ahadi, E, Rodriguez, AD, & Vahidi, S. Unraveling the mechanism of electrospray ionization. *Anal. Chem*. 2013; *85*(1):2–9.

Konijnenberg, A, Butterer, A, & Sobott, F. Native ion mobility-mass spectrometry and related methods in structural biology. *Biochim. Biophys. Acta - Proteins Proteomics* 2013;*1834*(6): 1239–1256.

Laguna, MTR, Medrano, R, Plana, MP, & Tarazona, MP. Polymer characterization by size-exclusion chromatography with multiple detection. *J. Chromatogr. A* 2001;*919*(1):13–19.

Lai, R, Dodds, ED, & Li, H. Molecular dynamics simulation of ion mobility in gases. *J. Chem. Phys*. 2018;*148*(6):064109.

Lanucara, F, Holman, SW, Gray, CJ, & Eyers, CE. The power of ion mobility-mass spectrometry for structural characterization and the study of conformational dynamics. *Nat. Chem*. 2014; *6*(4):281–294.

Lapthorn, C, Dines, TJ, Chowdhry, BZ, Perkins, GL, & Pullen, FS. Can ion mobility mass spectrometry and density functional theory help elucidate protonation sites in "small" molecules? *Rapid Commun. Mass Spectrom*. 2013;*27*(21):2399–2410.

Larriba, C, & Fernandez De La Mora, J. The gas phase structure of coulombically stretched polyethylene glycol ions. *J. Phys. Chem. B* 2012;*116*(1):593–598.

Larriba, C, & Hogan, CJ. Free molecular collision cross section calculation methods for nanoparticles and complex ions with energy accommodation. *J. Comput. Phys*. 2013;*251*:344–363.

Leach, AR. Molecular modelling principles. Pearson Education. 2001.

Larriba, C, De La Mora, JF, & Clemmer, DE. Electrospray ionization mechanisms for large polyethylene glycol chains studied through tandem ion mobility spectrometry. *J. Am. Soc. Mass Spectrom*. 2014;*25*(8):1332–1345.

Lee, JH, Pollert, K, & Konermann, L. Testing the robustness of solution force fields for MD simulations on gaseous protein ions. *J. Phys. Chem. B* 2019;*123*(31):6705–6715.

Lee, JW, Davidson, KL, Bush, MF, & Kim, HI. Collision cross sections and ion structures: Development of a general calculation method via high-quality ion mobility measurements and theoretical modeling. *Analyst* 2017;*142*(22):4289–4298.

Lehrle, RS, & Robb, JC. Direct examination of the degradation of high polymers by gas chromatography. *Nature* 1959;*183*(4676): 1671–1671.

Lemaur, V, Muccioli, L, Zannoni, C, Beljonne, D, Lazzaroni, R, Cornil, J, & Olivier, Y. On the supramolecular packing of high electron mobility naphthalene diimide copolymers: The perfect registry of asymmetric branched alkyl side chains. *Macromolecules* 2013;*46*(20):8171–8178.

Liénard, R, Duez, Q, Grayson, SM, Gerbaux, P, Coulembier, O, & De Winter, J. Limitations of ion mobility spectrometry-mass spectrometry for the relative quantification of architectural isomeric polymers: A case study. *Rapid Commun. Mass Spectrom*. 2020;*34*(S2):1–11.

Lloyd, PM, Suddaby, KG, Varney, JE, Scrivener, E, Derrick, PJ, & Haddleton, DM. A comparison between matrix-assisted laser desorption/ionisation time-of-flight mass spectrometry and size exclusion chromatography in the mass characterisation of synthetic polymers with narrow molecular-mass distributions: Poly (methyl methacrylate). *Eur. Mass Spectrom*. 1995;*1*:293–300.

Luo, M Du, Zhou, ZW, & Zhu, ZJ. The application of ion mobility-mass spectrometry in untargeted metabolomics: From separation to identification. *J. Anal. Test*. 2020;*4*(3):163–174.

Macha, SF, & Limbach, PA. Matrix-assisted laser desorption/ionization (MALDI) mass spectrometry of polymers. *Curr. Opin. Solid State Mater. Sci*. 2002;*6*(3):213–220.

Madorsky, SL, & Straus, S. Pyrolytic fractionation of polystyrene in a high vacuum and mass spectrometer analysis of some of the fractions. *J. Res. Natl. Bur. Stand*. 1948;*40*(5):417.

Mao, J, Zhang, B, Zhang, H, Elupula, R, Grayson, SM, & Wesdemiotis, C. Elucidating branching topology and branch lengths in star-branched polymers by tandem mass spectrometry. *J. Am. Soc. Mass Spectrom*. 2019;*30*(10):1981–1991.

Marklund, EG. Molecular self-occlusion as a means for accelerating collision cross-section calculations. *Int. J. Mass Spectrom*. 2015;*386*:54–55.

Marklund, EG, Degiacomi, MT, Robinson, C V., Baldwin, AJ, & Benesch, JLP. Collision cross sections for structural proteomics. *Structure* 2015;*23*(4):791–799.

Martens, JK, Compagnon, I, Nicol, E, McMahon, TB, Clavaguéra, C, & Ohanessian, G. Globule to helix transition in sodiated polyalanines. *J. Phys. Chem. Lett*. 2012;*3*(22):3320–3324.

Martin, SB. Gas chromatography: Application to the study of rapid degradative reactions in solids. *J. Chromatogr. A* 1959;*2*: 272–283.

Mayo, SL, Olafson, BD, & Goddard III, WA. DREIDING: A generic force field for molecular simulations. *J. Phys. Chem*. 1990; *94*(26):8897–8909.

McAllister, RG, Metwally, H, Sun, Y, & Konermann, L. Release of native-like gaseous proteins from electrospray droplets via the charged residue mechanism: Insights from molecular dynamics simulations. *J. Am. Chem. Soc*. 2015;*137*(39): 12667–12676.

Memboeuf, A, Vékey, K, & Lendvay, G. Structure and energetics of poly(ethylene glycol) cationized by Li+, Na+, K+ and Cs+: A first-principles study. *Eur. J. Mass Spectrom*. 2011;*17*(1):33.

Mesleh, MF, Hunter, JM, Shvartsburg, AA, Schatz, GC, & Jarrold, MF. Structural information from ion mobility measurements: Effects of the long-range potential. *J. Phys. Chem*. 1996;*100*(40):16082–16086.

Montaudo, G, Samperi, F, & Montaudo, MS. Characterization of synthetic polymers by MALDI-MS. *Prog. Polym. Sci*. 2006; *31*(3):277–357.

Morsa, D, Defize, T, Dehareng, D, Jérôme, C, & De Pauw, E. Polymer topology revealed by ion mobility coupled with mass spectrometry. *Anal. Chem*. 2014;*86*(19):9693–9700.

Morsa, D, Gabelica, V, & De Pauw, E. Effective temperature of ions in traveling wave ion mobility spectrometry. *Anal. Chem*. 2011;*83*(14):5775–5782.

Mottin, M, Souza, PCT, Ricci, CG, & Skaf, MS. CHARMM force field parameterization of peroxisome proliferator-activated receptor γ ligands. *Int. J. Mol. Sci*. 2017;*18*(1):15.

Van Mourik, T, Bühl, M, & Gaigeot, MP. Density functional theory across chemistry, physics and biology. *Philos. Trans. R. Soc. A Math. Phys. Eng. Sci*. 2014;*372*(2011):20120488.

Myers, CA, D'Esposito, RJ, Fabris, D, Ranganathan, S V., & Chen, AA. CoSIMS: An optimized trajectory-based collision simulator for ion mobility spectrometry. *J. Phys. Chem. B* 2019; *123*(20):4347–4357.

Paizs, B. A divide-and-conquer approach to compute collision cross sections in the projection approximation method. *Int. J. Mass Spectrom*. 2015;*378*:360–363.

Porrini, M, Rosu, F, Rabin, C, Darré, L, Gómez, H, Orozco, M, & Gabelica, V. Compaction of duplex nucleic acids upon native electrospray mass spectrometry. *ACS Cent. Sci*. 2017;*3*(5): 454-461.

Poyer, S, Comby-zerbino, C, Choi, CM, Macaleese, L, Bogliotti, N, Xie, J, Salpin, J, Dugourd, P, & Chirot, F. Conformational dynamics in ion mobility data. *Anal. Chem*. 2017;*89*(7): 4230–4237.

Prell, JS. Modelling collisional cross sections. In Comprehensive analytical chemistry (1st ed., Vol. *83*, pp. 1–22). Elsevier B.V. 2019.

Projected Superposition Approximation Webserver (http://psa.chem.fsu.edu/).

Pu, Y, Ridgeway, ME, Glaskin, RS, Park, MA, Costello, CE, & Lin, C. Separation and identification of isomeric glycans by selected accumulation-trapped ion mobility spectrometry-electron activated dissociation tandem mass spectrometry. *Anal. Chem*. 2016;*88*(7):3440–3443.

Pukala, TL, Ruotolo, BT, Zhou, M, Politis, A, Stefanescu, R, Leary, JA, & Robinson, C V. Subunit architecture of multiprotein assemblies determined using restraints from gas-phase measurements. *Structure* 2009;*17*(9):1235–1243.

Radell, EA, & Strutz, HC. Identification of acrylate and methacrylate: Polymers by gas chromatography. *Anal. Chem*. 1959; *31*(11):1890–1891.

Räder, HJ, & Schrepp, W. MALDI-TOF mass spectrometry in the analysis of synthetic polymers. *Acta Polym*. 1998;*49*:272–293.

Rayleigh, Lord. On the equilibrium of liquid conducting masses charged with electricity. *London, Edinburgh, Dublin Philos. Mag. J. Sci*. 1882;*14*(87):184–186.

Revercomb, HE, & Mason, EA. Theory of plasma chromatography/gaseous electrophoresis-A review. *Anal. Chem*. 1975;*47*(7): 970–983.

Rollins, K, Scrivens, JH, Taylor, MJ, & Major, H. The characterization of polystyrene oligomers by field-desorption mass spectrometry. *Rapid Commun. Mass Spectrom*. 1990;*4*(9): 355–359.

Ruotolo, BT, Benesch, JLP, Sandercock, AM, Hyung, S-J, & Robinson, C V. Ion mobility–mass spectrometry analysis of large protein complexes. *Nat. Protoc*. 2008;*3*(7):1139–1152.

Saintmont, F, De Winter, J, Chirot, F, Halin, E, Dugourd, P, Brocorens, P, & Gerbaux, P. How spherical are gaseous low charged dendrimer ions: A molecular dynamics/ion mobility study? *J. Am. Soc. Mass Spectrom*. 2020;*31*:8.

Sasanuma, Y. Conformational analysis of poly(propylene oxide) and its model compound 1,2-dimethoxypropane. *Macromolecules* 1995;*28*(25):8629–8638.

Schulten, H -R, & Lattimer, RP. Applications of mass spectrometry to polymers. *Mass Spectrom. Rev*. 1984;*3*(2):231–315.

Shrivastav, V, Nahin, M, Hogan, CJ, & Larriba-Andaluz, C. Benchmark comparison for a multi-processing ion mobility calculator in the free molecular regime. *J. Am. Soc. Mass Spectrom*. 2017;*28*(8):1540–1551.

Shvartsburg, AA, & Jarrold, MF. An exact hard-spheres scattering model for the mobilities of polyatomic ions. *Chem. Phys. Lett*. 1996;*261*(1–2):86–91.

Shvartsburg, AA, Mashkevich, S V., Baker, ES, & Smith, RD. Optimization of algorithms for ion mobility calculations. *J. Phys. Chem. A* 2007;*111*(10):2002–2010.

Sinclair, E, Hollywood, KA, Yan, C, Blankley, R, Breitling, R, & Barran, P. Mobilising ion mobility mass spectrometry for metabolomics. *Analyst* 2018;*143*(19):4783–4788.

Snyder, SR, & Wesdemiotis, C. Elucidation of low molecular weight polymers in vehicular engine deposits by multidimensional mass spectrometry. *Energy and Fuels* 2021;*35*(2):1691–1700.

Soltani, S, Oh, MI, & Consta, S. Effect of solvent on the charging mechanisms of poly(ethylene glycol) in droplets. *J. Chem. Phys*. 2015;*142*(11):114307.

Stojko, J, Fieulaine, S, Petiot-Bécard, S, Van Dorsselaer, A, Meinnel, T, Giglione, C, & Cianférani, S. Ion mobility coupled to native mass spectrometry as a relevant tool to investigate extremely small ligand-induced conformational changes. *Analyst* 2015;*140*(21):7234–7245.

Sun, Y, Vahidi, S, Sowole, MA, & Konermann, L. Protein structural studies by traveling wave ion mobility spectrometry: A critical look at electrospray sources and calibration issues. *J. Am. Soc. Mass Spectrom*. 2015;*27*(1):31–40.

Tanaka, K, Waki, H, Ido, Y, Akita, S, Yoshida, Y, Yoshida, T, & Matsuo, T. Protein and polymer analyses up to m/z 100 000 by laser ionization time-of-flight mass spectrometry. *Rapid Commun. Mass Spectrom*. 1988;*2*(8):151–153.

Tatro, SR, Baker, GR, Fleming, R, & Harmon, JP. Matrix-assisted laser desorption/ionization (MALDI) mass spectrometry: Determining Mark-Houwink-Sakurada parameters and analyzing the breadth of polymer molecular weight distributions. *Polymer (Guildf)*. 2002;*43*(8):2329–2335.

Tintaru, A, Chendo, C, Wang, Q, Viel, S, Quéléver, G, Peng, L, Posocco, P, Pricl, S, & Charles, L. Conformational sensitivity of conjugated poly(ethylene oxide)-poly(amidoamine) molecules to cations adducted upon electrospray ionization–A mass spectrometry, ion mobility and molecular modeling study. *Anal. Chim. Acta* 2014;*808*:163–174.

Tonelli, AE. PLLA in solution: A flexible random-coil or an extended, rather rigid helical polymer. *Macromolecules* 2014; *47*(17):6141–6143.

Tonnelé, C, Champagne, B, Muccioli, L, & Castet, F. Nonlinear optical contrast in azobenzene-based self-assembled monolayers. *Chem. Mater*. 2019;*31*(17):6759–6769.

Trimpin, S, & Clemmer, DE. Ion mobility spectrometry/mass spectrometry snapshots for assessing the molecular compositions of complex polymeric systems. *Anal. Chem*. 2008;*80*(23):9073–9083.

Trimpin, S, Plasencia, M, Isailovic, D, & Clemmer, DE. Resolving oligomers from fully grown polymers with IMS-MS. *Anal. Chem*. 2007;*79*(21):7965–7974.

Ude, S, Fernández De La Mora, J, & Thomson, BA. Charge-induced unfolding of multiply charged polyethylene glycol ions. *J. Am. Chem. Soc*. 2004;*126*(38):12184–12190.

Uetrecht, C, Rose, RJ, van Duijn, E, Lorenzen, K, & Heck, AJR. Ion mobility mass spectrometry of proteins and protein assemblies. *Chem. Soc. Rev*. 2010;*39*(5):1633–1655.

Veale, CGL, Mateos Jimenez, M, Mackay, CL, & Clarke, DJ. Native ion mobility mass spectrometry reveals that small organic acid fragments impart gas-phase stability to carbonic anhydrase II. *Rapid Commun. Mass Spectrom*. 2020;*34*(2):1–8.

Völlmin, J, Kriemler, P, Omura, I, Seibl, J, & Simon, W. Structural elucidation with a thermal fragmentation-Gas chromatography-Mass spectrometry combination. *Microchem. J*. 1966;*11*(1):73–86.

Wall, LA. Mass spectrometric investigation of the thermal decomposition of polymers. *J. Res. Natl. Bur. Stand*. 1948;*41*(4):315–322.

Wang, D, Chen, K, Kulp, JL, & Arora, PS. Evaluation of biologically relevant short α-helices stabilized by a main-chain hydrogen-bond surrogate. *J. Am. Chem. Soc*. 2006;*128*(28):9248–9256.

Wei, M, Gao, Y, Li, X, & Serpe, MJ. Stimuli-responsive polymers and their applications. *Polym. Chem*. 2017;*8*(1):127–143.

Weidner, SM, & Trimpin, S. Mass spectrometry of synthetic polymers. *Anal. Chem*. 2010;*82*(12):4811–4829.

Weiser, LJ, & Santiso, EE. A CGenFF-based force field for simulations of peptoids with both cis and trans peptide bonds. *J. Comput. Chem*. 2019;*40*(22):1946–1956.

Wesdemiotis, C. Multidimensional mass spectrometry of synthetic polymers and advanced materials. *Angew. Chemie Int. Ed*. 2017;*56*(6):1452–1464.

Wesdemiotis, C, Nilüfer, S, Polce, MJ, Dabney, DE, Chaicharoen, K, & Katzenmeyer, BC. Fragmentation pathways of polymer ions. *Mass Spectrom. Rev*. 2011;*30*(4):523–559.

De Winter, J, Lemaur, V, Ballivian, R, Chirot, F, Coulembier, O, Antoine, R, Lemoine, J, Cornil, J, Dubois, P, Dugourd, P, & Gerbaux, P. Size dependence of the folding of multiply charged sodium cationized polylactides revealed by ion mobility mass spectrometry and molecular modelling. *Chem. - A Eur. J*. 2011;*17*(35):9738–9745.

Wyttenbach, T, Von Helden, G, & Bowers, MT. Conformations of alkali ion cationized polyethers in the gas phase: Polyethylene glycol and bis[(benzo-15-crown-5)−15-ylmethyl] pimelate. *Int. J. Mass Spectrom. Ion Process*. 1997;*165-166*:377–390.

Yamashita, M, & Fenn, JB. Electrospray ion source. Another variation on the free-jet theme. *J. Phys. Chem*. 1984;*88*(20): 4451–4459.

Zanotto, L, Heerdt, G, Souza, PCT, Araujo, G, & Skaf, MS. High performance collision cross section calculation-HPCCS. *J. Comput. Chem*. 2018;*39*(21):1675−1681.

AUTHOR BIOGRAPHIES

Quentin Duez received his PhD in Chemistry from the University of Mons (Belgium) in 2020. His graduate research, under the joint supervision of Profs. Pascal Gerbaux and Jérôme Cornil, focused on the structural analysis of synthetic polymers by ion mobility mass spectrometry and molecular modelling. He is now a postdoctoral researcher in the group of Prof. Jana Roithová in the Radboud University (The Netherlands). His current research aims to study reaction intermediates by mass spectrometry, ion mobility spectrometry and ion spectroscopy.

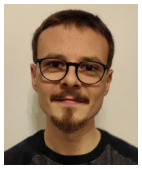

Sébastien Hoyas obtained a MSc in chemistry from the Université de Mons (UMONS) in June 2017. In October 2017, he started a PhD at UMONS on the structural characterization of peptoids by combining theoretical chemistry and ion mobility spectrometry coupled to mass spectrometry, under the supervision of Profs. Jérôme Cornil and Pascal Gerbaux (CMN and S²MOs).

Thomas Josse received his PhD degree in Science, under the supervision of Prof Pascal Gerbaux and Dr Olivier Coulembier from the University of Mons, Belgium in 2015, where he studied the synthesis and characterization of cyclic polymers obtained by mean of ring-closure and ring-expansion approaches. He is now R&D scientist at Materia Nova research center, in charge of projects related to polymeric and composite materials.

Jérôme Cornil received a PhD in Chemistry from the University of Mons-Hainaut (Belgium) in 1996 under the supervision of Jean-Luc Brédas. He did postdoctoral stays at the University of California at Santa Barbara (with A.J. Heeger) and at MIT Boston (with R.S. Silbey). He is research director of the Belgian National Fund for Scientific Research (FNRS) since 2012. His research interests mostly deal with the theoretical characterization at the atomistic level of the structural and electronic properties of organic and hybrid materials in the isolated state, in their bulk or at interfaces.

Pascal Gerbaux has obtained his PhD in Science from the University of Mons-Hainaut in 1999 under the supervision of Prof Robert Flammang. After having completed several postdoctoral stays abroad, that is, Ecole Polytechnique de Palaiseau, University of Washington and University of Utrecht, he got a permanent position at the University of Mons as a F.N.R.S. Senior Research Associate. For years, his research topics are related to the study of gas phase ions using mass spectrometry methods. He is now Full Professor of organic chemistry and mass spectrometry and head of the Organic Synthesis and Mass Spectrometry Laboratory at UMONS.

Julien De Winter obtained his PhD from the University of Mons in 2011 under the supervision of Prof. Pascal Gerbaux and Prof. Philippe Dubois. His main research areas are the synthesis of original macromolecules/polymers and their in-depth studies by mass spectrometry. He did some scientific stays on different topics, for example, about Ion Mobility Spectrometry (Lyon, France), polymer synthesis (Warwick University, UK), rotaxane synthesis (University of Manchester, UK). Since January 2015, he is Junior Lecturer at the University of Mons in the laboratory of Prof. Pascal Gerbaux and is responsible for the use and development of mass spectrometry methods for macromolecular characterization.

How to cite this article: Duez Q, Hoyas S, Josse T, Cornil J, Gerbaux P, De Winter J. Gas-phase structure of polymer ions: Tying together theoretical approaches and ion mobility spectrometry. *Mass Spectrometry Reviews*, 2021; e21745. https://doi.org/10.1002/mas.21745